Passenger Vehicle-Powered Two Wheeler Pre-Crash Trajectory Reconstruction and Conflict Analysis Results for Real-World Crashes in the EU and US and its Application to Advanced Crash Avoidance Technologies

R. Michael Van Auken
Dynamic Research Inc.
United States of America

John Lenkeit
Dynamic Research Inc.
United States of America

Terry Smith
Dynamic Research Inc.
United States of America

Scott Kebschull
Dynamic Research Inc.
United States of America

Paper Number 19-0096

ABSTRACT

Research Question / Objective: Advanced Driver Assistance Systems (ADASs) such as Forward Collision Warning have been developed for light passenger vehicles (LPVs) to avoid and mitigate collisions with other road users and objects. These technologies may have contributed to a reduction in LPV traffic fatalities in the EU and US. However the number of powered two wheeler (PTW) fatalities has remained relatively constant in the US. To fully realize the potential safety benefits across all vehicle categories, LPV crash avoidance technologies also need to be effective in avoiding collisions with PTWs. To accomplish this, knowledge of the pre-crash LPV-PTW vehicle trajectories and conflicts is needed to guide the development and testing of effective crash countermeasures for both LPVs and PTWs.

Methods and Data Sources: Crash scenario database development tools previously developed to evaluate LPV-LPV crash countermeasure effectiveness have been extended to LPV-PTW crash scenarios. This involved using information for a large sample of LPV-PTW crashes from the EU Motorcycle Accidents In-Depth Study (MAIDS) and US Motorcycle Crash Causation Study (MCCS) databases, which are based on in-depth crash investigations and the Organisation for Economic Co-operation and Development (OECD) Common Methodology. The vehicle pre-crash trajectories were estimated based on the coded data and digitized information from the scaled pre-crash scene diagrams. The pre-crash conflict state was then analyzed based on these trajectories.

Results: The estimated pre-crash trajectories using this method indicate that LPV-PTW pre-crash trajectories and conflicts in France, Germany, Italy, and the US have many similarities, but there are some differences as well. These results indicate that conflicts in several types of pre-crash scenarios, such as the LPV turning across the PTW path in the same direction or opposite direction, begin less than 1.5 sec before impact, which may not be sufficient time for some crash countermeasures based on conflict detection and driver warnings to be effective.

Discussions and Limitations: The accuracy of the results is based on a number of assumptions, approximations, and limitations in the data and methods used. These include the accuracy and representativeness of the data based on in-depth crash investigations, as well as the domain-of-validity and accuracy of the vehicle directional control models used.

Conclusion and relevance to session submitted: Analysis of real world accident data is critical to the development and evaluation of ADAS and automated driving systems. This analysis has shown that LPV-PTW crash countermeasures need to function with shorter pre-crash conflict epochs, or in the pre-conflict phase, in order

to be effective in preventing collisions. This information may help to define requirements for LPV-PTW crash countermeasures (e.g., C-ITS V2V and Blind Spot Detection), evaluate their effectiveness, and inform the development of performance confirmation tests (e.g., New Car Assessment Programs).

INTRODUCTION

Advanced Driver Assistance Systems (ADASs) such as Forward Collision Warning (FCW), Automatic Emergency Braking (AEB), and Blind Spot Warning (BSW) have been developed for Light Passenger Vehicles (LPVs) to avoid and mitigate collisions with other road users and objects. These crash avoidance and mitigation countermeasures may have contributed to the 41% reduction in the overall number fatalities in the EU from 43,151 in 2007 to 25,651 in 2016 [1], and a 9% reduction in the overall number of traffic fatalities in the US from 41,259 to 37,461 in the same time period [2]. A main component of these overall reductions were a 42% reduction in LPV occupant fatalities in the EU from 20,744 to 11,990, and an 18% reduction in the US from 29,072 to 23,714. Powered two wheeler (PTW) fatalities, comprising mopeds and motorcycles,[1] also decreased by 42% from 7,522 in 2007 to 4,334 in 2016 in the EU, but increased by 2% in the US over the same period. In an effort to explain the differences in the PTW versus LPV fatality trends in the US, one question is whether or not LPV ADASs are as effective in avoiding collisions with PTWs compared to other road users.

Lenkeit and Smith [4] evaluated the ability of eight 2016 model year LPVs equipped with FCW to detect an exemplar motorcycle and passenger car using two tests in the US National Highway Traffic Safety Administration (NHTSA) FCW confirmation test procedures. The results of this preliminary evaluation indicated that only two of the eight LPVs tested were able to pass the NHTSA test procedure scenario with a stationary motorcycle as the principal other vehicle (POV), compared to all LPVs passing the test with a stationary passenger car as the POV. Therefore these preliminary results tend to indicate that FCW systems may not be as effective in avoiding or mitigating collisions with a motorcycle as they are with a passenger car.

Van Auken et al. ([5],[6],[7]) then estimated the pre-crash trajectories and conflicts for 101 crashes in the US and 266 crashes in the EU involving one LPV and one PTW. This analysis was based on the European Motorcycle Accidents In-Depth Study (MAIDS) database [8] and the US Federal Highway Administration's (FHWAs) Motorcycle Crash Causation Study (MCCS) database [9]. Both of these databases were developed based on in-depth accident investigations using methodology based on the Organisation for Economic Co-operation and Development (OECD) Common Methodology [10].

Analysis of these estimated pre-crash trajectories indicated that the conflicts begin later, and therefore with smaller Time to Collision (TTC) values, compared to results for some LPV-LPV crashes. Therefore there may be less time for a driver or crash avoidance technology to avoid or mitigate a LPV-PTW crash after a conflict has been detected, compared to a LPV-LPV crash. As a result such systems may be less effective in avoiding LPV-PTW crashes.

Background

Dynamic Research, Inc. (DRI) has been developing and applying safety impact analysis methods for many years (e.g., [11]). This included the development of a comprehensive Safety Impact Methodology (SIM) in two Honda-DRI Advanced Crash Avoidance Technology (ACAT) programs for the US NHTSA. The comprehensive and general structure of this methodology and accompanying tools are well suited for the potential evaluation of LPV ADAS (e.g., FCW, AEB, and BSW) effectiveness in avoiding and/or mitigating collisions with PTWs with the extensions originally outlined in [12], as well as other applications such as pre-crash conflict analysis, the development of system requirements, and testing.

In-Depth LPV-PTW Crash Databases

Two databases that have sufficient suitable information to be integrated into this SIM methodology are from the European MAIDS study and the US MCCS study. Both of these studies had coded accident data and crash scene diagrams based on in-depth investigations.

[1] Powered Two Wheelers comprise L1 and L3 vehicles as defined in [3]. L1 vehicles are commonly known as mopeds. L3 vehicles are commonly known as motorcycles. See the Definitions/Abbreviations Section.

The MAIDS study was conducted from 1998 through 2002 by the European Association of Motorcycle Manufacturers (ACEM) with co-funding by the European Commission. It was developed using the OECD Common Methodology [10]. All of the cases are from France, Germany, Italy, Netherlands, and Spain. Most of the MAIDS cases are from the 1999 to 2001 calendar year time period.

The MCCS study was conducted by a team from Oklahoma State University, Westat, and Dynamic Sciences, Inc. and sponsored by the Federal Highway Administration (FHWA). It was also developed based the OECD Common Methodology with adaptions to the US motorcycling conditions. All of the cases are from Orange County, California. All of the MCCS cases are from the 2011 to 2015 calendar year time period.

Project Aims

The objective of this project was to extend the SIM tools and data to include the MAIDS and MCCS data in order to better understand the pre-crash conflicts of LPV-PTW crashes, to guide the development of LPV ADASs in avoiding and mitigating collisions with a PTW, and to evaluate their effectiveness and benefits.

SAFETY AREA TO BE ADDRESSED BY THE ADVANCED TECHNOLOGIES

The objective of the ACAT SIM with the PTW extensions is to evaluate the effectiveness and benefits of LPV ADASs (e.g., FCW, AEB and BSW) in avoiding or mitigating LPV-PTW crashes. It is assumed that these technologies could address crashes where the LPV driver inattention is a contributing factor, but may also be applicable to safety-relevant cooperative ITS (C-ITS) and other technologies as well.

The size of the problem to be addressed

One of the first steps in the development and evaluation a crash avoidance technology is to determine the size of the traffic safety problem in terms of broadly defined non-technology specific crash types. The estimated numbers of fatalities that represent the size of the problem for the entire EU and US motor vehicle fleets in the 2016 calendar year by the crash category and type of vehicle involved are listed in Table 1. Some of these crashes are not expected to be addressable by specific LPV technologies such as AEB due to either the vehicle application (e.g., not an LPV), the vehicle role (e.g., struck vehicle), or other technology relevant factors. For example, the results in Table 1 indicate there were 997 PTW fatalities in the EU involving only one vehicle (i.e., did not involve an LPV). These results also indicate that there were 3,337 PTW fatalities in the EU involving one or more other vehicles, which account for 13% of all traffic fatalities in the EU. There were also 3,273 PTW fatalities in the US involving one or more other vehicles, which account for 9% of all US traffic fatalities in the US. A large portion of these cases involve an LPV, which could be potentially addressed by an LPV ADAS.

Table 1. Estimated crash problem size for the entire EU and US motor vehicle fleets in the 2016 calendar year

(A)	(B)	(C)	(D)	(E)	(F)	(G)
Crash Category	**Number of EU Fatalities[a]**			**Number of US Traffic Fatalities[b]**		
	PTW	Other =(D)-(B)	Total	PTW	Other =(G)-(E)	Total
1 Vehicle	997[c]	6,658	7,655[d]	2,065	18,415	20,480
2+ Vehicle	3,337[e]	14,659	17,996[e]	3,273	14,053	17,326
Total	4,334[f]	21,317	25,651[g]	5,338	32,468	37,806

Sources:

[a] Based on EU Community database on road accidents (CARE) data.

[b] Based on US Fatality Analysis Reporting System (FARS, [13]) data (2018-05-18) query.

[c] Assumed equal to 23% of all PTW fatalities based on [14], p 10, Table 5. It is assumed that none of the single vehicle crashes are pedal cycles.

[d] [14], p 10, Table 5.

[e] =Total- Single Vehicle

[f] [1], p 19, Table 6 (677 moped fatalities) and p 20, Table 7 (3,657 motorcycle fatalities).

[g] [1], p 10, Table 2.

METHODS

The analytical approach involved refining and applying the methods developed in [5],[6],[7] for the EU MAIDS and US MCCS databases. The MAIDS and MCCS databases were developed using similar, but not identical, in-depth crash investigation methods. The MAIDS database was developed according the OECD common methodology. The MCCS database was developed using a methodology incorporating both the OECD and NHTSA methods.

Overview of the Crash Scenario Database Development Tools

A conceptual block diagram of the crash scenario database tools is given in Figure 1. These tools are collectedly referred to as "Module 1" in the Honda/DRI ACAT SIM. These Module 1 tools construct a harmonized crash scenario database for use in the development and evaluation of ADASs (e.g., requirements, simulation, and testing). The inputs are archival accident data such as the MAIDS and MCCS data as indicated at the top of the figure. The resulting crash scenario database comprises text summaries (to the extent available), harmonized coded data, scene diagrams, crash geometry and pre-crash time histories as depicted by the shaded database in Figure 1. These tools are organized into three sub-modules as follows:

- Submodule 1.1 assembles a crash scenario database with a representative sample of LPVs involved in real-world crashes. Ideally the crash scenario database would include all types of crashes and severities, which could be weighted to represent all crashes involving a LPV. This sub-module extracts cases from various coded accident databases such the MAIDS and MCCS data [8],[9].
- Submodule 1.2 is a tool to download or extract crash scene diagrams for each case in the crash scenario database if available.
- Submodule 1.3 is an Automated Accident Reconstruction Tool (AART) to reconstruct the pre-crash and crash position versus time trajectories of the LPVs for each case in the crash scenario file, provided there is sufficient information available and the case is within the domain-of-validity of the AART (e.g., there is a crash scene diagram, vehicle velocity, and contact information). The resulting reconstructions can be used for simulation and testing. These results can also be used for other analyzes, such as the identification of pre-crash conflicts described in [6].

The extensions of these tools for the US MCCS and EU MAIDS data were described in [5],[6],[7].

The results described herein are based on 367 cases from the US, France, Germany, and Italy that were reconstructed using this tool. The distribution of these cases is depicted in Figure 2. Each of these cases had sufficient information in the coded data, crash scene diagram, and supporting documentation to reconstruct the case. This excluded cases where a suitable scene diagram not available or did not have sufficient information about the locations of the vehicles prior to the impact and at the point of impact.

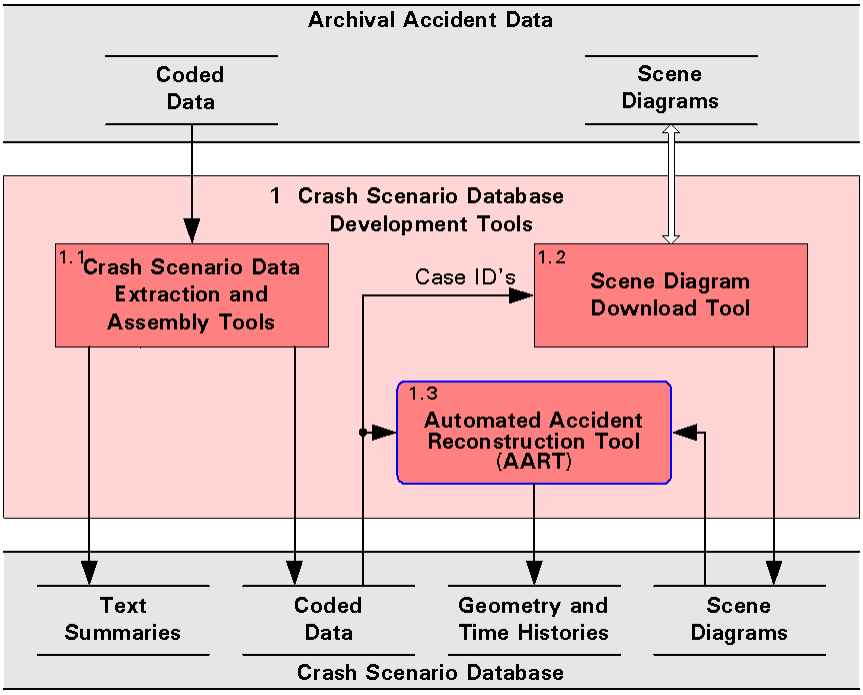

Figure 1. Crash Scenario Database Development Tools (e.g., [11]).

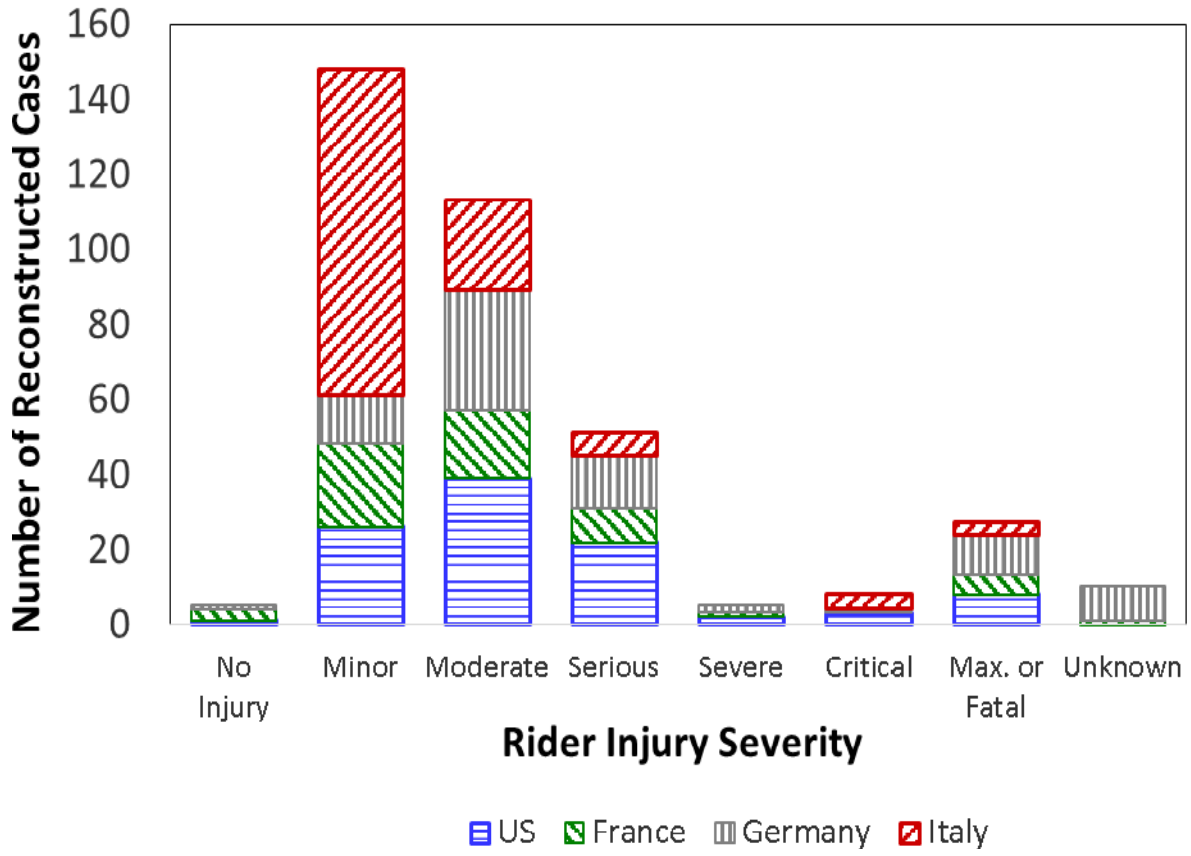

Figure 2. Number of reconstructed Cases by rider injury severity and country.

Extensions for the Current Results

The results presented herein are based on the following further refinements of the data and methods:

- Module 1.1
  - The NASS Accident Type described in Appendix A was coded for both vehicles in each of the reconstructed cases. The coded variables are VATYPE for the LPV and PATYPE for the PTW according to the conventions used in Appendix F of [11]. Reconstructed cases with similar crash types were then classified into the 24 different crash configuration groups listed in Table 2.
  - Data indicating if "*view obstructions* [were] *present and contributed to accident causation*," were extracted from the MAIDS and MCCS databases for both the LPV driver and PTW rider in order to further classify the reconstructed cases.
- Module 1.3 (Motorcycle Automated Accident Reconstruction Tool – M-AART)
  - The assumed pre-crash vehicle speeds in cases where the coded travel speed was missing or unknown to take into account coded data indicating the vehicle was traveling at a constant speed or accelerating.
  - Numerous refinements to the trajectory estimation algorithms to improve the accuracy of the estimated trajectories based on the available data. This includes new "reference trajectory" types with constant steer input rates or rider lean angle rates, which are consistent with the white process noise inputs assumed by the Kalman Filter-Smoother, provided there a are sufficient number of digitized pre-crash vehicle positions. The reference trajectories are initial solutions to the vehicle equations of motion that are used to determine locally linearized equations for the Kalman Filter-Smoother (e.g., [5]). It was also required that the PTW speed was either always less than or always greater than the critical speed of the Weir-Zellner model [16].[2] This avoids a singularity in the quasi-steady reference trajectory solution at the critical speed.

Table 2. Crash Configuration Groups based on NASS Accident Types

Crash Configuration Group based on NASS Accident Types		NASS Accident Types
Mnemonic	**Description**	**VATYPE/PATYPE**
HO/ODSS	Head-on or opposite direction side swipe	50/51, 51/50, 65/64
LPV LTAP/LD	LPV left turn across PTW path/lateral direction	82/83
LPV LTAP/OD	LPV left turn across PTW path/opposite direction	68/69
LPV LTAP/SD	LPV left turn across PTW path/same direction	72/73
LPV LTIP	LPV left turn into PTW path/same direction	76/77
LPV RE	LPV rear-end PTW	20/21, 24/25, 24/26, 28/29
LPV RTAP/SD	LPV right turn across PTW path/same direction	70/71
LPV RTIP/SD	LPV right turn into PTW path/same direction	78/79
LPV UT	LPV U-turn across PTW path	940/941…944
PTW LTAP/LD	PTW left turn across LPV path/lateral direction	83/82
PTW LTAP/OD	PTW left turn across LPV path/opposite direction	69/68
PTW LTAP/SD	PTW left turn across LPV path/same direction	73/72
PTW LTIP	PTW left turn into LPV path	77/76
PTW RE	PTW rear-end LPV	21/20, 25/24, 26/24, 29/28, 30/28
PTW RTAP/SD	PTW right turn across LPV path/same direction	71/70
PTW RTIP/OD	PTW right turn into LPV path/opposite direction	81/80
PTW RTIP/SD	PTW right turn into LPV path/same direction	79/78
SCP/L	Straight crossing path, PTW on left side of LPV	86/87, 89/88
SCP/R	Straight crossing path, PTW on right side of LPV	87/86, 88/89
SDSS/L	Same direction side swipe, PTW on the left of LPV	47/45
SDSS/R	Same direction side swipe, PTW on the right of LPV	46/45
T2/OD	Both vehicles turning/opposite direction	68/82
T2/SD	Both vehicles turning/same direction	76/78, 78/76
Other	Other	74/74, 98/98

[2] The "Norton 850" parameter values in [16] were assumed for motorcycles and the "Moped B" parameter values in [17] were assumed for mopeds.

Pre-Crash Conflict State Estimation

As previously described in [6], the state of conflict between the LPV and PTW can be estimated as a function of time before the impact based on the estimated vehicle trajectories. For the purpose of this analysis the conflict state C at time t was defined for $t \le t_{\text{impact}}$ as follows: $C(t) \triangleq \text{true}$ if the vehicles will contact each other at time t_{contact} if their linear and angular velocities remain constant between time t and t_{contact}; otherwise $C(t) \triangleq \text{false}$ if the vehicles will never contact.[3] For practical considerations the contact evaluation time interval was limited to up to 1 sec after the reconstructed impact time (i.e., $t \le t_{contact} \le t_{impact} + 1\text{sec}$). This definition can include momentary benign conflicts that may occur several sec before impact in addition to the final conflict, as illustrated by the example in Figure 4 and Figure 5. Of interest is the when the final conflict begins.[4]

RESULTS

The results in this section describe the estimated trajectories and conflicts for two example cases, followed by a summary for all of the cases.

Example pre-crash trajectories and state of conflict

Example Head-On Case

An example pre-crash trajectory reconstruction of a Head-On case is illustrated in Figure 3, Figure 4, and Figure 5. This case involves a moped overtaking two other PTWs and then impacting a LPV that was exiting a parking area and turning to the right onto the roadway. The coded data indicates that there were rider "*view obstructions present that contributed to accident causation*." Presumably these view obstructions were the other motorcycles. Figure 3 shows the pre-crash vehicle speeds that were assumed based on coded data. Figure 5 shows the estimated vehicle directional control inputs versus time. Figure 4 shows the resulting vehicle trajectories overlaid on the crash scene diagram. The vehicle trajectories were fit to the locations of the LPV and moped shown on the scene diagram. The estimated vehicle positions and orientations are depicted at 1 sec intervals and the movement of the cg positions are depicted by continuous curves. The control inputs and vehicle positions when $C(t) = \text{true}$ are shown highlighted in yellow. The LPV and PTW vehicle level NASS accident types illustrated in Appendix A that best describe this case were VATYPE=51 and PATYPE=50 respectively, and therefore the HO/ODSS crash configuration group according to Table 2.

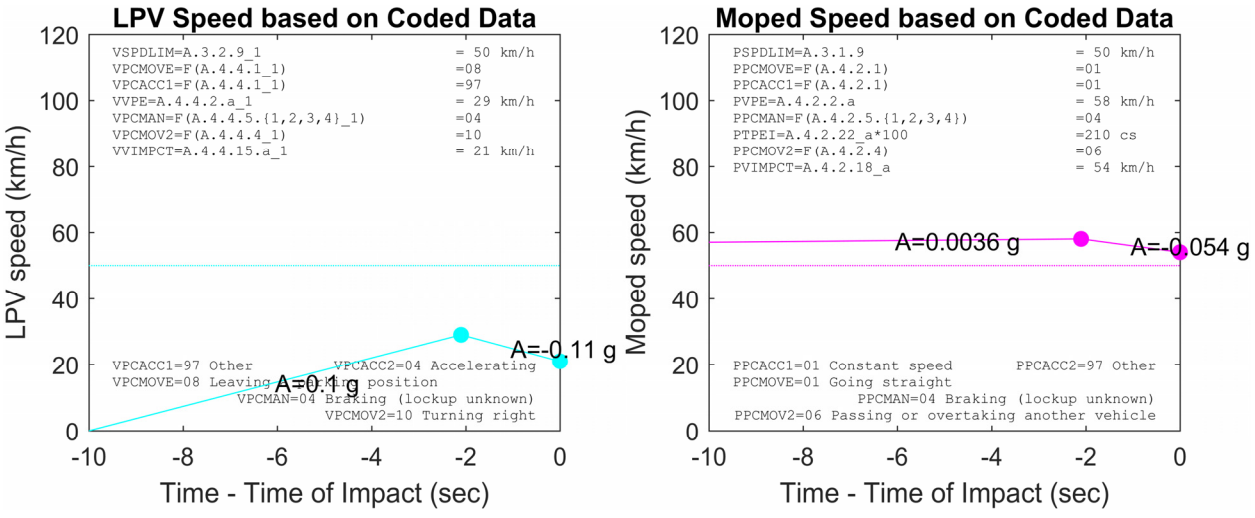

Figure 3. Assumed pre-crash speeds versus time for the exemplar head-on case based on coded data.

[3] The PTW handlebars were included in the potential contact with the LPV. It was assumed that the handlebars were 0.89 m wide for the purpose of this conflict analysis.

[4] See footnote 9 in [6] for addition background and rationale for this conflict definition.

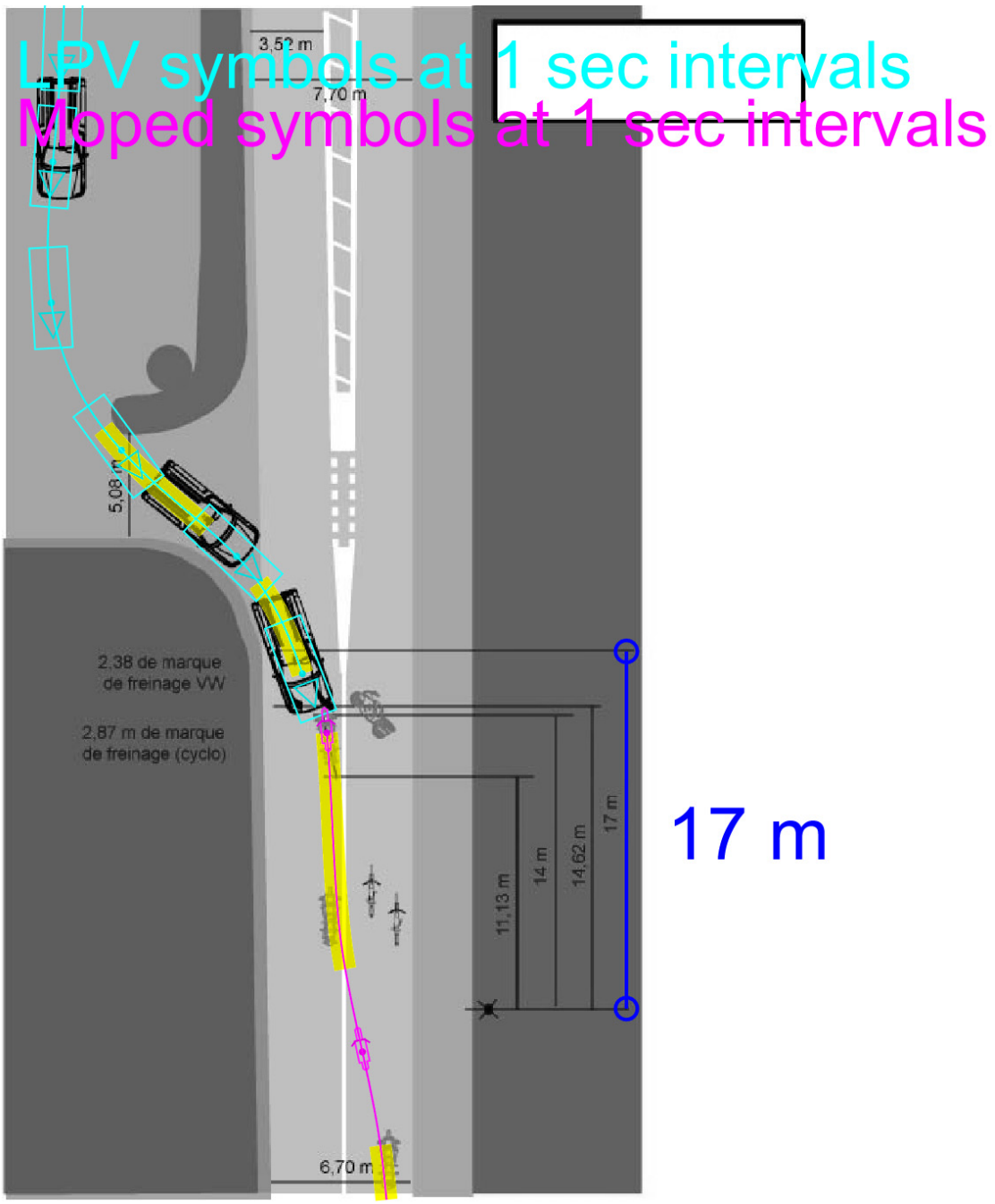

Figure 4. Estimated pre-crash trajectories for the examplar head-on case.

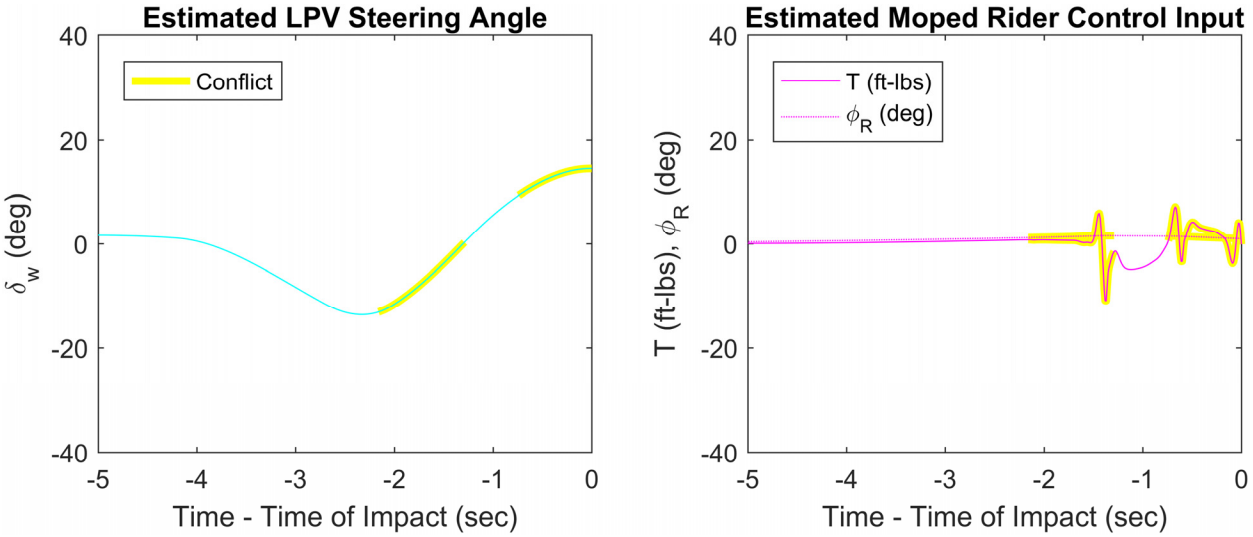

Figure 5. Directional control inputs versus time for the exemplar head-on case.

This example case illustrates the directional responses of the LPV and PTW to the vehicle control inputs. It was assumed for this case that the moped was traveling at approximately 7 km/h above the posted speed limit of 50 km/h 10 sec prior to impact.[5] At the same time a LPV was leaving a parked position. The M-AART estimated that the driver turned to the left (negative steer angle) to approach the roadway, then turned to the right (positive steer angle) to merge onto the roadway going in the opposite direction to the PTW. At the time of the coded precipitating event, 2.1 sec before impact, the coded data indicates the PTW was traveling at a constant speed of 58 km/h, and the LPV had accelerated to 29 km/h, as indicated in Figure 3. The rider then passed to the left of two other PTWs traveling in the same direction. The estimated rider passing maneuver involved first applying positive steer torque to turn to the left, then negative steer torque to turn to the right, then positive torque to recover as depicted in Figure 5. The coded data indicates both vehicles braked and the coded impact speeds were 21 km/h and 54 km/h respectively. Figure 4 shows the close agreement between the estimated vehicle trajectories and the available information. The maximum differences between the digitized LPV and PTW positions and the corresponding estimated trajectories are 0.7 m and 0.5 m respectively.

This example also illustrates both a momentary conflict which is benign and the final conflict which resulted in impact. The benign conflict occurs between t=-2.2 sec and t=-1.3 sec. This is when the LPV is headed towards the roadway and the vehicle velocity vectors intersect. The risk of collision will be small if the LPV turns to merge onto the roadway and the both vehicles stay within their respective lanes. This benign conflict ends as expected when the LPV turns to merge onto the roadway. The final conflict then begins 0.7 sec before impact. This is after the PTW crosses the lane boundary into the PTWs path. The coded data for this cases also indicates that the moped operator's view of the LPV was obstructed.

Example case with both vehicles turning

Another example pre-crash trajectory reconstruction is illustrated in Figure 6. This case involves a motorcycle turning left across the LPV path while the LPV is also turning left to follow the main roadway. Therefore both vehicles are turning left. The maximum differences between the digitized LPV and PTW positions and the corresponding estimated trajectories are 0.6 m and 0.2 m respectively. The estimated trajectories are in a state of conflict beginning 1.6 sec prior to impact. The coded data indicates that that there were LPV driver and PTW rider "*view obstructions present that contributed to accident causation*." Therefore the conflict may not have been detected because of visual obstructions. The LPV and PTW vehicle level NASS accident types illustrated in Appendix A that best describe this case were VATYPE=68 and PATYPE=82 respectively, and therefore the "T2/OD" crash configuration group according to Table 2.

[5] The coded data for this case indicate that the moped had enhanced motor power and a modified exhaust.

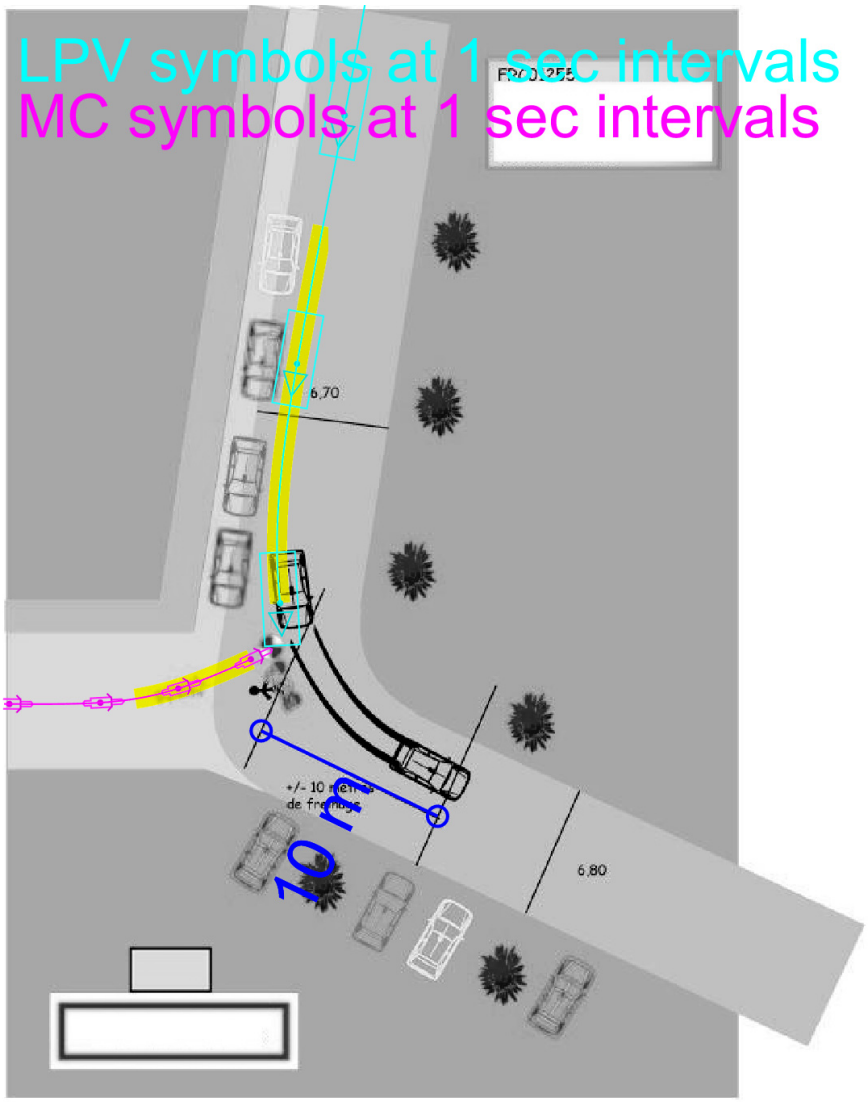

Figure 6. Estimated pre-crash trajectories and conflict for an exemplar case with both vehicles turning.

Pre-crash LPV-PTW trajectories

The estimated trajectories for the 367 reconstructed cases are summarized in Figure 7 through Figure 12. Figure 7 and Figure 8 show the results for the 266 EU MAIDS cases and 101 US MCCS data side by side. Figure 9 and Figure 10 show the results for the 242 cases involving a motorcycle and 125 cases involving a moped side by side. Figure 11 and Figure 12 show the results without and with a coded visual obstruction that contributed to the accident causation. Figure 7, Figure 9, and Figure 11 show the estimated PTW trajectories relative to the LPV in the LPV reference frame. The dotted lines show the relative positions of the PTW cg at 0.1 sec time intervals for the 3 sec prior to impact. Therefore pre-crash trajectories with higher velocities have larger spacing between the dots compared to trajectories with lower velocities. Likewise Figure 8, Figure 10, and Figure 12 show the estimated LPV trajectories relative to the PTW in the PTW reference frame. The relative vehicle positions when the conflict state $C(t) = \text{true}$ are highlighted in yellow.

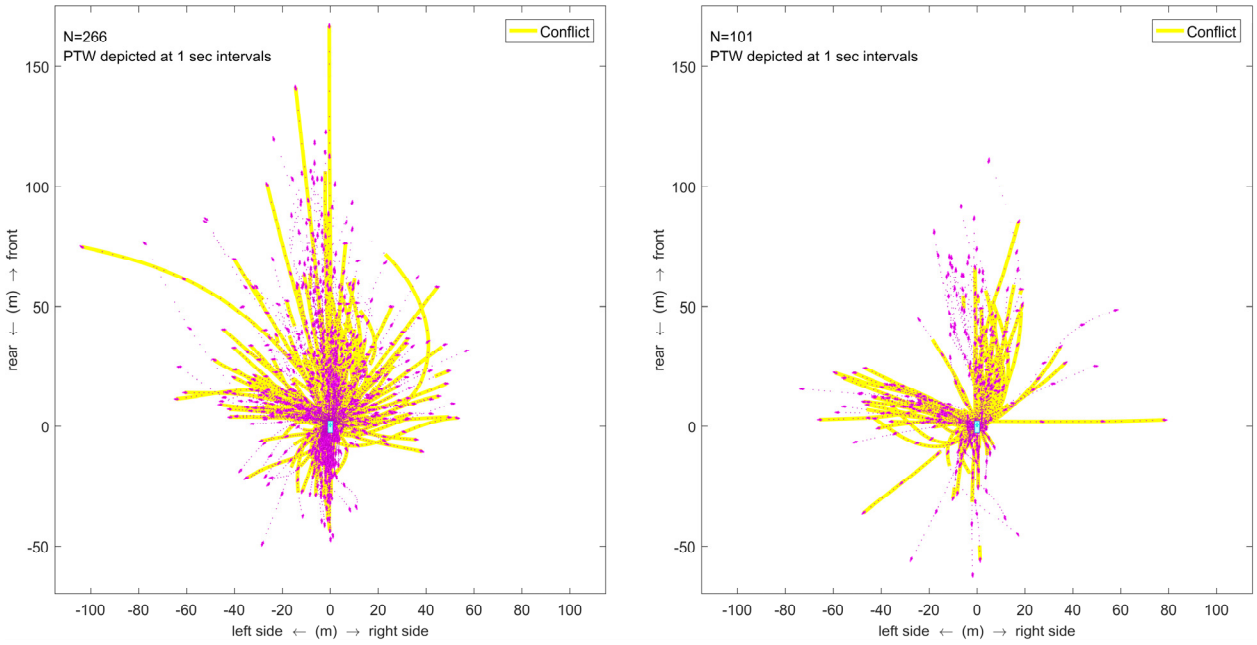

Figure 7. Estimated PTW trajectories and conflicts relative to the LPV for the 3 sec prior to impact by region (266 EU MAIDS cases on the left versus 101 US MCCS cases on the right).

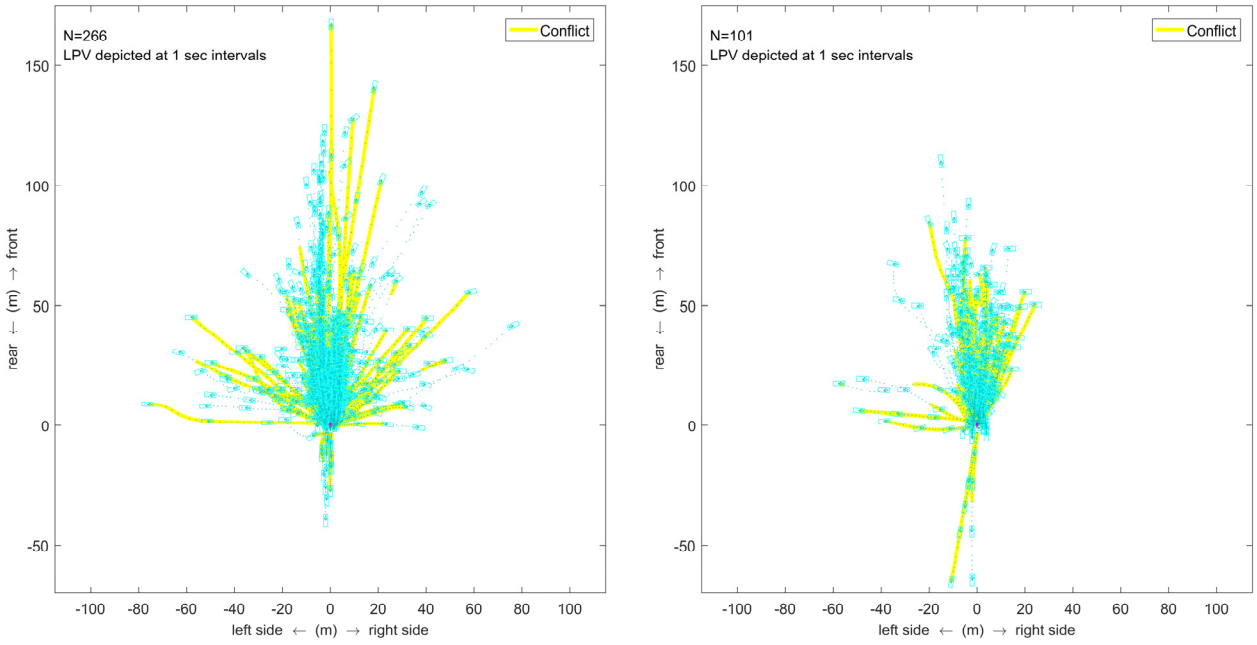

Figure 8. Estimated LPV trajectories and conflicts relative to the PTW for the 3 sec prior to impact by region (266 EU MAIDS cases on the left versus 101 US MCCS cases on the right).

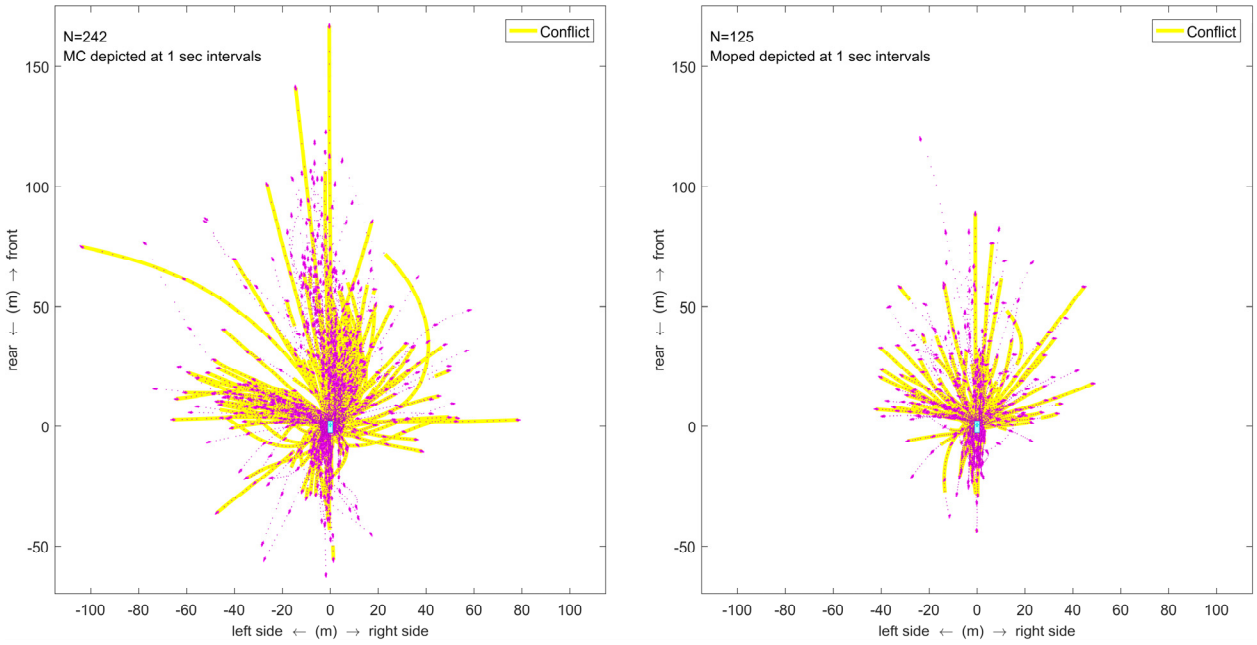

Figure 9. Estimated PTW trajectories and conflicts relative to the LPV for the 3 sec prior to impact by PTW type (242 motorcycle cases on the left versus 125 moped cases on the right).

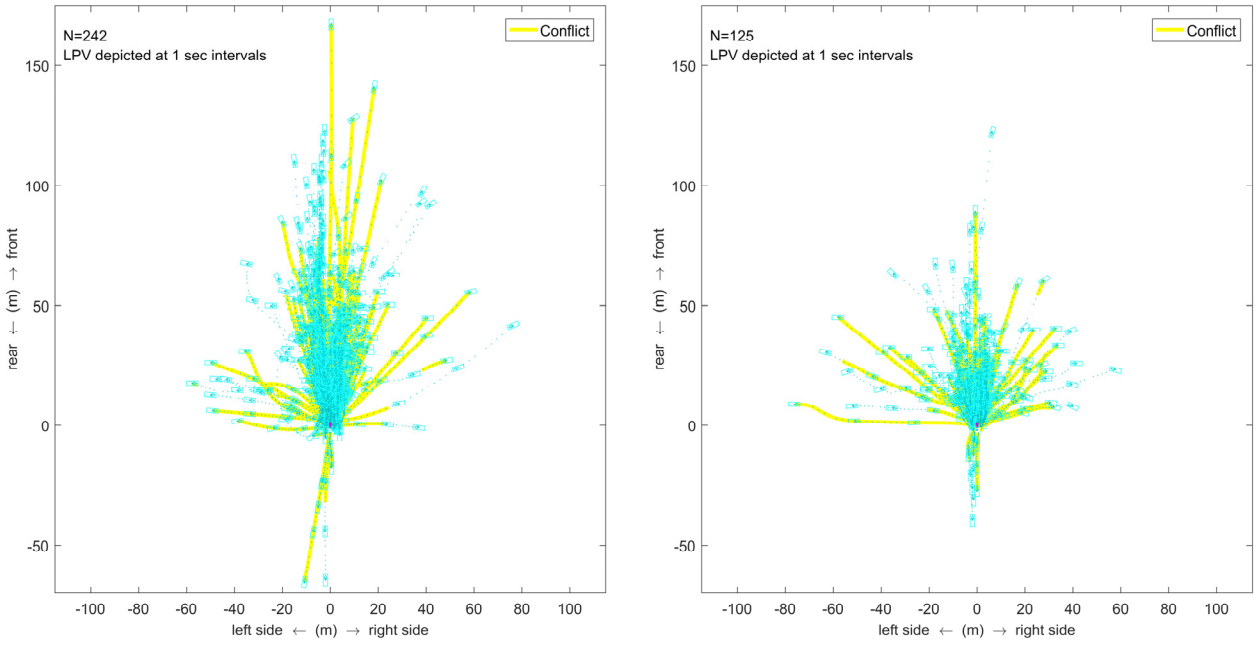

Figure 10. Estimated LPV trajectories and conflicts relative to the PTW for the 3 sec prior to impact by PTW type (242 motorcycle cases on the left versus 125 moped cases on the right).

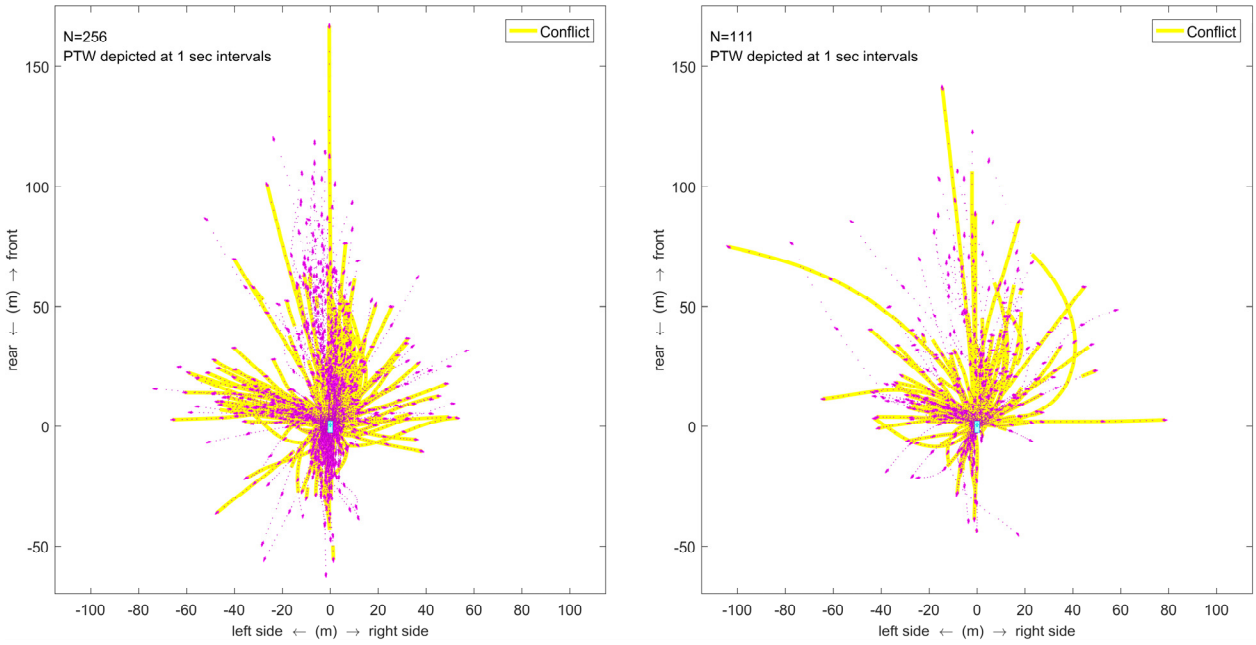

Figure 11. Estimated PTW trajectories and conflicts relative to the LPV for the 3 sec prior to impact by visual obstruction (256 cases without visual obstruction on the left versus 111 cases with visual obstruction on the right).

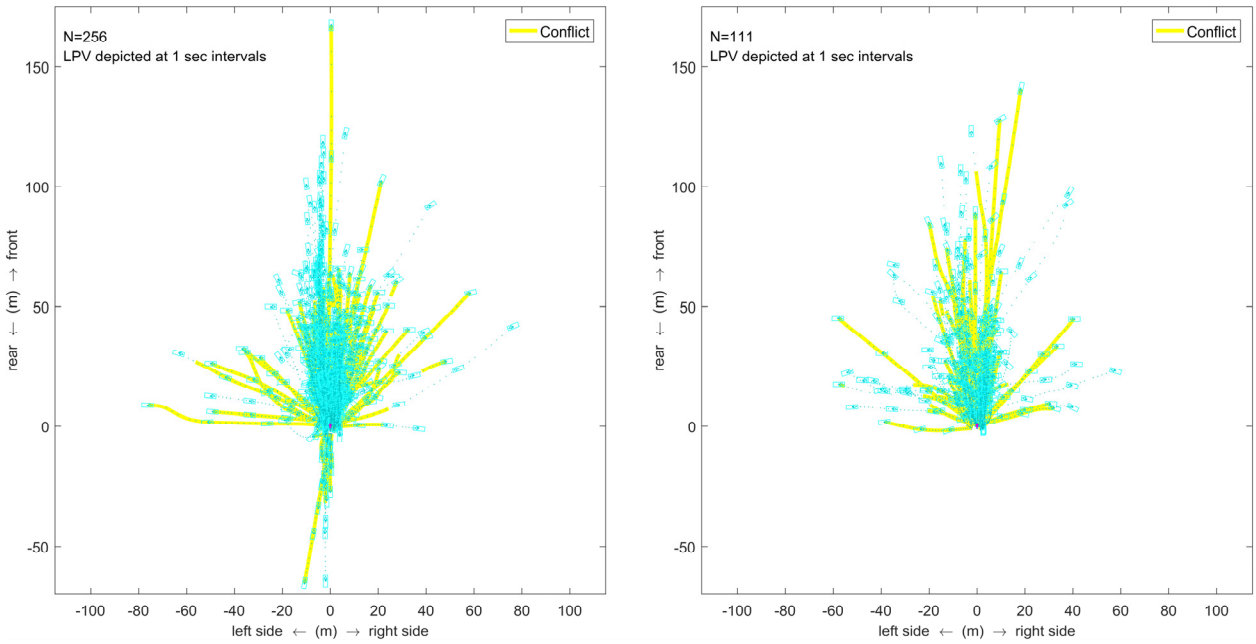

Figure 12. Estimated LPV trajectories and conflicts relative to the PTW for the 3 sec prior to impact by visual obstruction (256 cases without visual obstruction on the left versus 111 cases with visual obstruction on the right).

The results in Figure 7 and Figure 8 compare the 266 EU MAIDS cases and the 101 US MCCS cases. These results indicate that the some of the EU cases have higher relative pre-crash closing velocities than the US cases. These results also indicate that the EU cases are more broadly distributed in relative approach angle than the US cases. The

smaller distribution of US cases compared to the EU cases may be partially attributed to the smaller US sample size. The US cases are primarily from a suburban sampling region with very few cases on rural roads or limited access divided highways. The EU cases were also sampled ten years before the US cases.

The results in Figure 9 and Figure 10 compare the 242 cases involving a MC to the 125 cases involving a moped. All but one of the moped cases are from the MAIDS database. These results indicate that the LPV-MC cases tend to have higher relative closing velocities than the LPV-moped cases, which is consistent with moped speed restrictions in the EU. The differences are most apparent in the longitudinal direction in the PTW reference frame. Both the MC and moped cases have a wide distribution of relative approach angles.

The results in Figure 11 and Figure 12 compare the 111 cases that had a coded visual obstruction that contributed to the conflict to the 256 cases that did not. The most noticeable difference is that none of the PTW rear-end LPV cases had a visual obstruction. This suggests that these PTW rear-end LPV cases may involve rider distraction or other factors.

Pre-crash LPV-PTW conflicts

The highlighted conflict state results in Figure 9 to Figure 12 indicate that many of the conflicts begin less than 3 sec before impact. The median start time for the MAIDS and MCCS data are 1.4 sec and 1.6 sec before impact respectively, and approximately 1.4 sec before impact overall.

The distributions of the conflict start times by crash configuration group and PTW type are illustrated in Figure 13. The crash configuration groups on the horizontal axis of this graph are defined in terms of the NASS accident type according to Table 2. The pre-crash trajectories and conflicts for each of these crash configuration groups are depicted in Appendix B. The vertical axis of this graph is the estimated conflict start time relative to the time of impact, which is a negative value. The vertical range of each box in this figure represents the 25th and 75th percentile values for the conflict start time, and the horizontal line in each box represents the median value. The number of cases for each crash configuration group are indicated by the numerical value shown above the median in each box. The graph is limited to the 5 sec epoch before impact because earlier conflict times are increasingly sensitive to the assumed vehicle speeds and estimated vehicle trajectories (many of which were extrapolated backwards in time before the digitized vehicle positions in the scene diagrams). The last 1.5 sec before impact are indicated by a light red shaded background. This shading represents the epoch where there may be insufficient time for the driver or rider to react to an ADAS warning in order to mitigate or avoid the crash, and therefore the countermeasures involving simple conflict detection and driver warning may not be effective.[6]

The results in Figure 13 indicate 10 of 21 crash configuration groups with median conflict times that began less than 1.5 sec before impact. The six largest of these groups are the LPV LTAP/OD (90 cases), LPV LTAP/SD (29), LPV UT (22), PTW RE (22), HO/ODSS (20), and LPV RTAP/SD (19), which combined represent 55% (202/367) of the reconstructed cases. The 15 cases in the other four crash configuration groups all involve the PTW turning.

[6] According to Neale and Dingus, "[w]hen a driver is looking forward, driver reaction time averages about 1.5 seconds and may be as high as 2.5 or 3.0 seconds in all but the most extreme cases" [15].

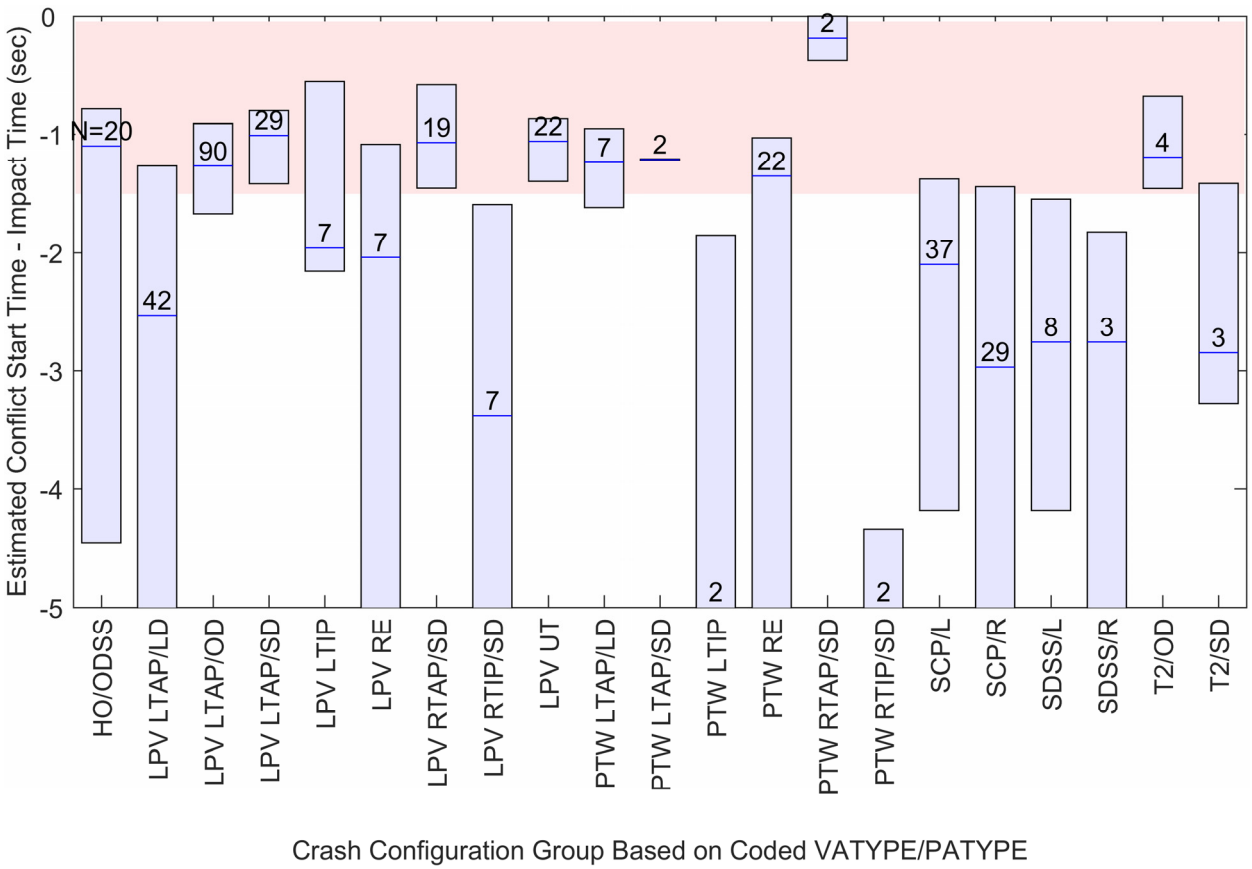

Figure 13. Distributions of estimated LPV-PTW conflict start times by crash configuration group.

Comparison of EU MAIDS and US MCCS cases

The estimated conflict start times are compared in further detail by data source in Figure 14. The format of Figure 14 is similar to Figure 13, but each crash configuration bar is split into pairs. The results for the EU MAIDS cases are depicted by the cyan colored boxes on the left, and the results for the US MCCS cases are depicted by the magenta colored boxes on the right.

The relative frequency of the MAIDS and MCCS cases were compared using a Pearson chi-square test. The resulting p-value=0.06 suggests that the relative frequencies of the MAIDS and MCCS cases are different, but the difference is not statistically significant at the 0.05 level.

The mean conflict start times for each pair were also compared using two-sample t-tests. The t-tests assumed that the start times in each sample are normally distributed with homogenous variance. Therefore only crash configuration groups with four or more cases were tested (i.e., two or more statistical degrees-of-freedom). The only crash configuration group with a statistically significant difference in the mean conflict start time is the LPV LTAP/OD group (p-value<0.01). This statistically significant difference is attributed to the large number of cases (90).

These results indicate that there are some differences between the two data sets, but that these differences are primarily related to the differences in the numbers of cases in each crash type rather than differences within each group. In other words, the conflict times within each crash configuration group are similar because they relative trajectories within each group are similar, as depicted in Appendix B. For example, there are more than 10 MAIDS and 10 MCCS cases in each of the LPV LTAP/LD, LPV LTAP/OD, and SCP/L groups, and the MAIDS and MCCS results for these groups are similar. Therefore we assumed that the two datasets can be combined without substantially changing the conclusions regarding conflict start times by crash configuration group.

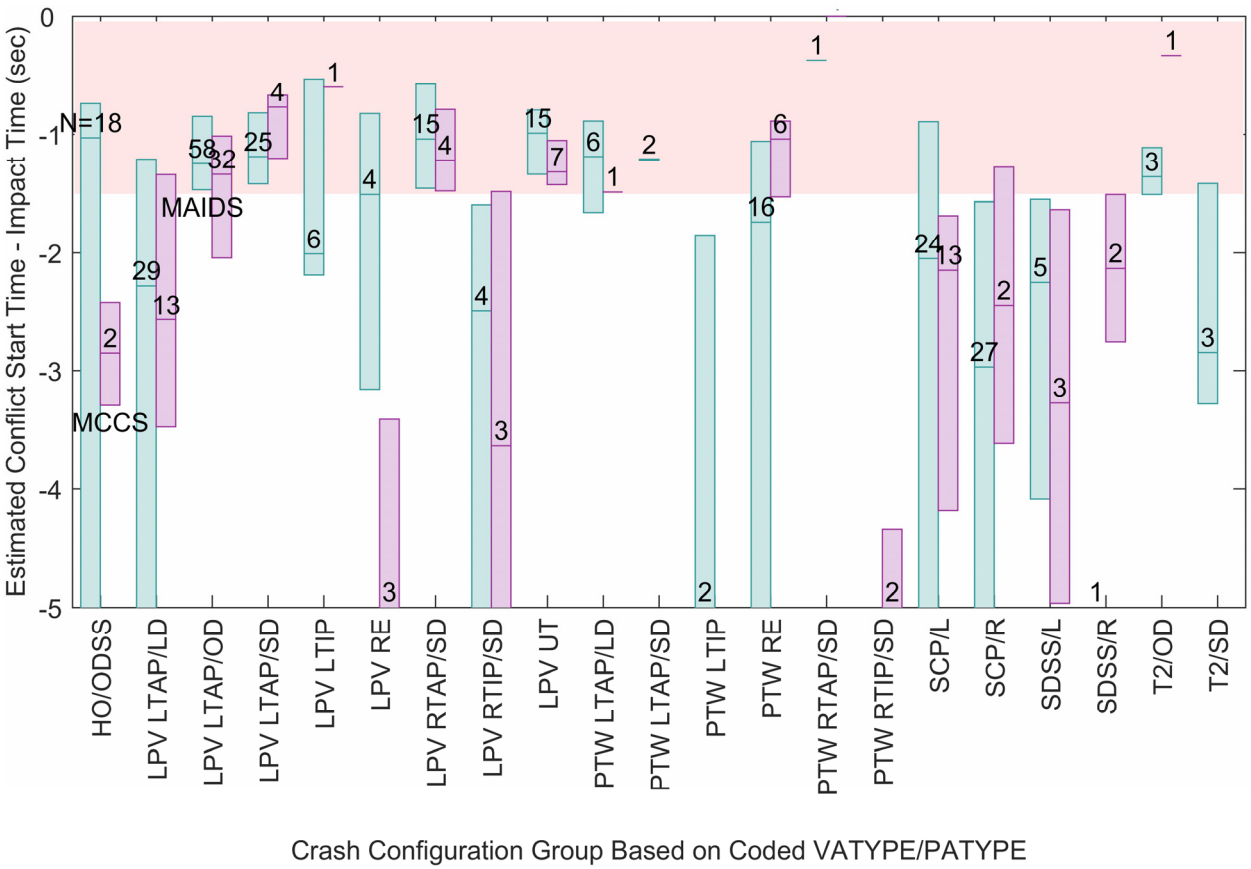

Figure 14. Estimated LPV-PTW conflict start times by crash configuration group and data source.

Comparison by PTW Type

Likewise the results in Figure 15 compare the estimated conflict start time results by PTW type. The format of Figure 15 is similar to Figure 14 but the paired bars are different. The results for motorcycles are depicted by cyan boxes on the left, and the results for mopeds are depicted by magenta boxes on the right.

The relative frequency of the MC and moped cases were also compared using a Pearson chi-square test. The resulting p-value=0.03 indicates that the relative frequencies of the MC and moped cases are statistically significantly different at the 0.05 level. However if the US MCCS cases are excluded, the resulting p-value is 0.37, which is not statistically significant.

The mean conflict start times for the MC and moped in each crash configuration group were also compared using t-tests. None of the groups had a statistically significant differences between the mean MC and moped conflict start times.

These results also indicate that the main differences between the MC and moped crash configurations are due to relative differences in sampling frequency, which may be attributed to difference in the US and EU, but the conflict start times are similar. There are more than 10 MC and 10 moped cases in each of the five LPV LTAP and SCP groups, and the MC and moped results in four of these groups are similar. Therefore we assumed that the two PTW types can be combined without substantially changing the conclusions about the conflict start time results for each crash configuration group.

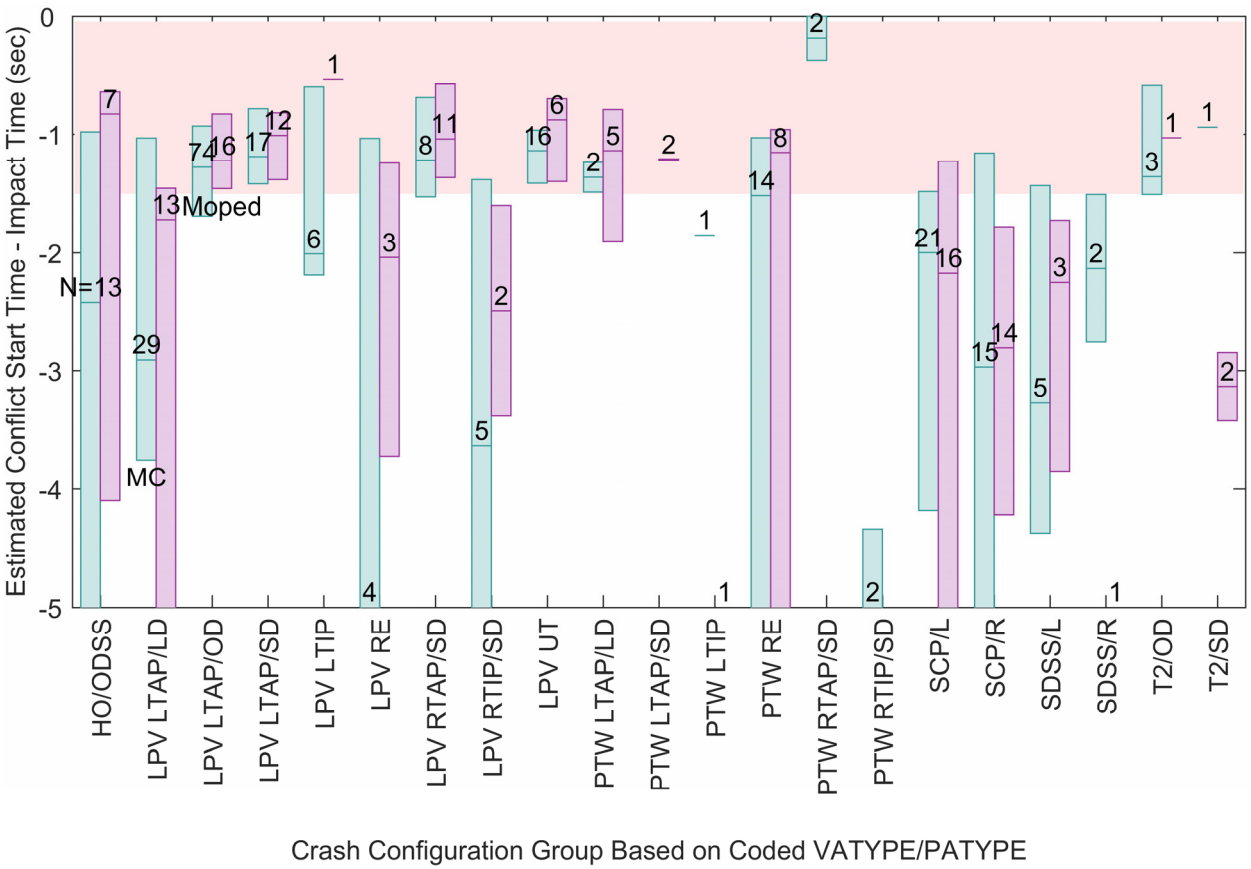

Figure 15. Estimated LPV-PTW conflict start times by crash configuration group and PTW type.

Comparison by Visual Obstruction

The results in Figure 16 compare the estimated conflict start time results by whether or not the coded data indicated that "*view obstructions were present and contributed to accident causation.*" The results in the cyan boxes on the left are without any visual obstruction, and the results in the magenta boxes on the right are with a view obstruction for either the LPV driver, PTW rider, or both. None of the crash configuration groups had a statistically significant difference in the mean conflict start times by visual obstruction, but the differences in the relative number of cases were statistically significantly different (p-value<0.01).

Most (86) of the 111 cases involving a visual obstruction were in the six HO/ODSS, LPV LTAP, and SCP crash configuration groups. There were 247 cases in these six groups combined, and 35% had a coded visual obstruction.

Nearly all (74) of the 79 cases in the LPV LTIP (6), rear end (7+20), RTAP/SD (18+2), and U-turn (21) groups did not have a coded visual obstruction. Therefore other factors such as operator distraction or error may be contributing to these types of crashes. It is unknown how many of the 22 U-turns were legal or not. The HO/ODSS, LPV LTAP/OD and LPV LTAP/SD groups had short conflict epochs regardless of whether or not there was a visual obstruction.

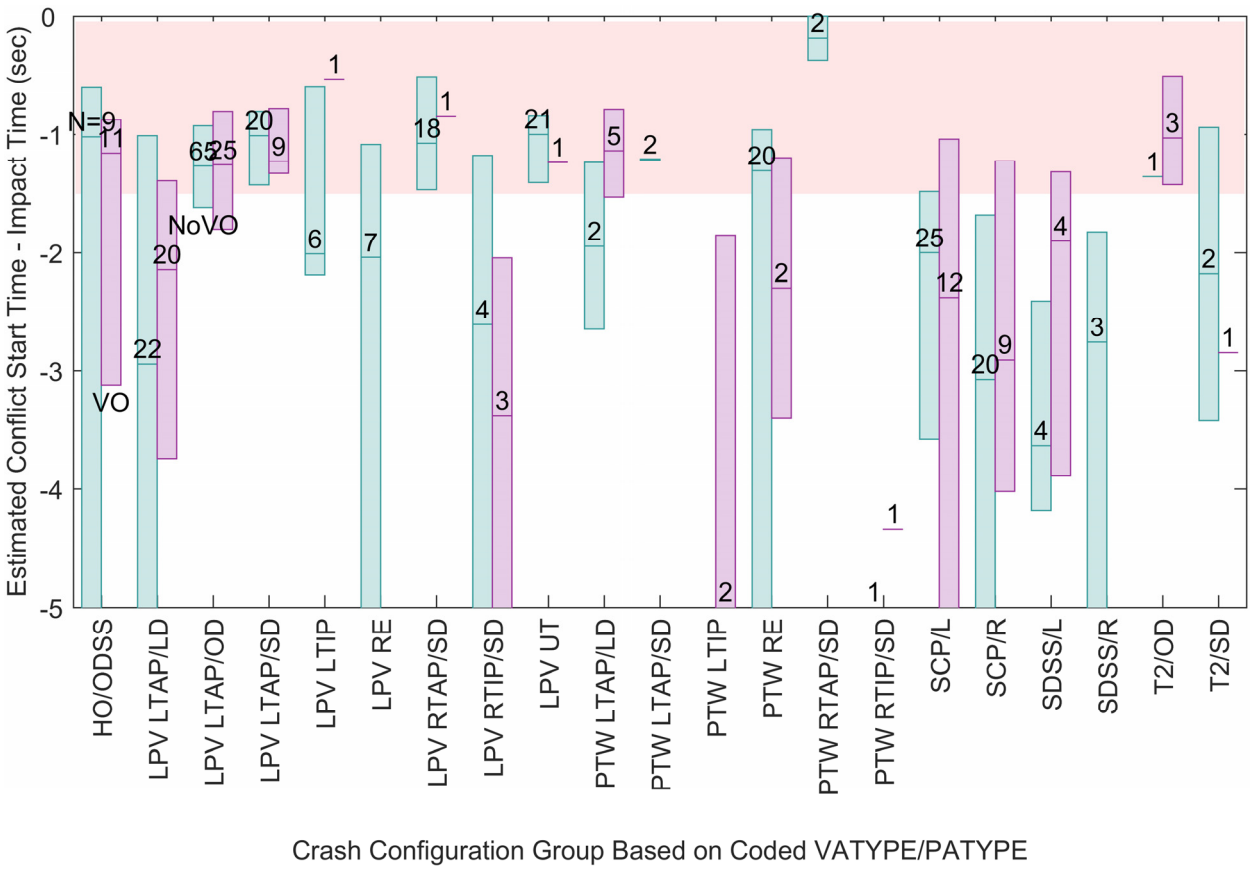

Figure 16. Estimated LPV-PTW conflict start times by crash configuration group and visual obstruction.

DISCUSSION

The effectiveness of potential conflict and crash countermeasures may depend on how soon the conflict is detected before impact. For comparison, the results in Figure 17 illustrate the distribution of conflict start times and collision effectiveness (CE) results for different technology relevant crash types (TRCTs) from a previous ADAS evaluation reported in [18]. The results for the "Primary" TRCT for which the crash avoidance countermeasure was intended to address, and three "secondary" TRCTs in which the technology designer thought the system might also be effective. A CE value of 0 indicates the technology is not effective in avoiding any of the crashes, which is undesirable. A CS value of 1 indicates the technology completely eliminates all of the crashes with the crash type, which is desirable. These results indicate that the crash avoidance countermeasure tends to be more effective for TRCTs with earlier conflict start times. Similar effectiveness results were observed in [11],[19].[7]

[7] The collision effectiveness results in Figure 17 are based on simulated cases that have been weighted to represent the US fleet in the 2009 calendar year. The conflict start times are based on the unweighted unique cases in the simulation sample. Results for the other secondary TRCTs are not shown due to insufficient numbers of reconstructable cases for the evaluation reported in [18].

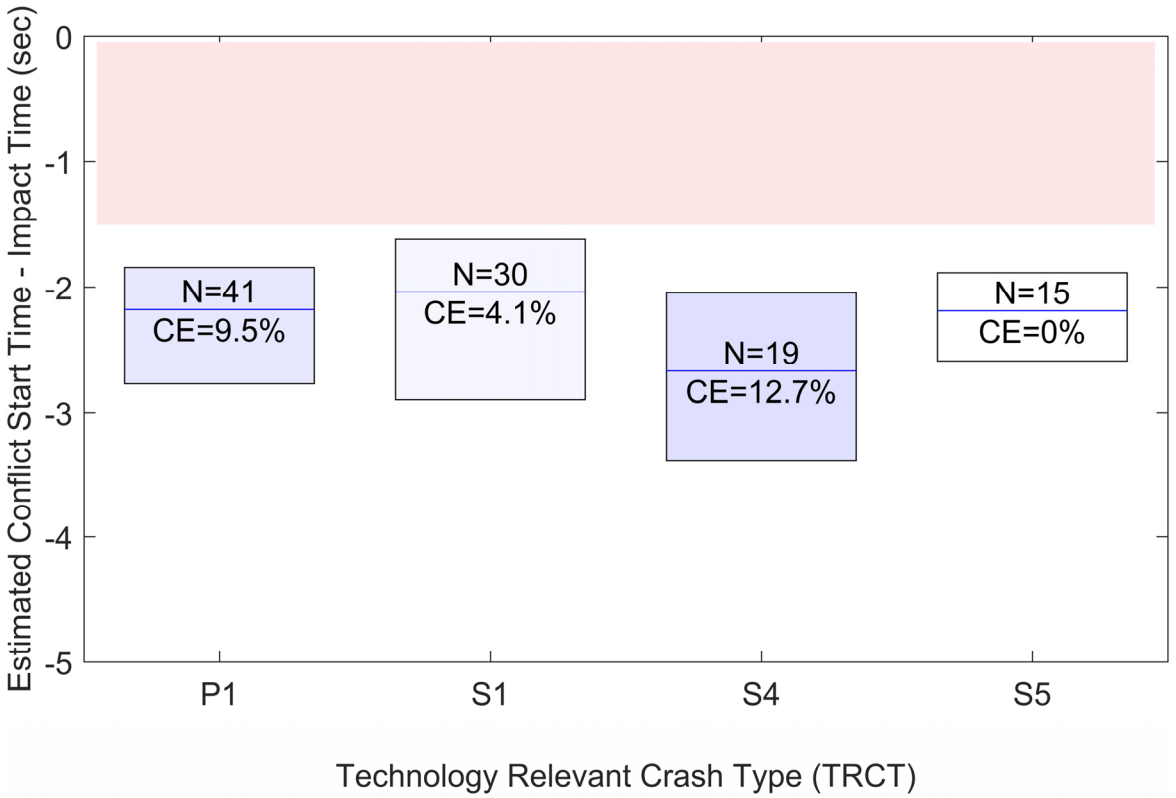

Figure 17. Boxplot distributions of estimated LPV-LPV conflict start times for a pre-production crash avoidance technology.

As previously described, the results in Figure 13 indicate several crash configuration groups with short pre-crash conflict times. The quartile and median times for the 90 LPV LTAP/OD cases were 0.9, 1.3, and 1.7 sec before impact respectively. The results in Figure B3 indicate that the cases from the front left tended to have short conflict times, and there would have been insufficient time to detect and warn the driver before a collision

The quartile and median times for the 29 LPV LTAP/SD cases were 0.8, 1.0, and 1.4 sec before impact respectively. The results in Figure B4 indicate many cases where the PTW may have been in the LPV blind spot during the conflict. However a BSW system might not have been able to detect a conflict and warn the driver with sufficient time to avoid a collision.

Other potential countermeasures could be ADASs such as AEB that are not affected by the driver response time, or by detecting and warning the driver about the impending conflict sooner. The conflict could be detected sooner by changing the vehicle "contact" criteria to include close encounters or use more advanced sensors and algorithms. However this could also result in false alarms, which is undesirable.

Impending conflicts could also be detected sooner and avoided or mitigated if the vehicle operators can see each other and properly communicate their intended paths before the conflict starts. One way to achieve this is by maximizing visual scanning strategies and vehicle conspicuity, and proper use and detection of turn signals. This could also be enhanced by safety-relevant cooperative C-ITS V2V communications systems such as Motorcycle Approach Indication (MAI) and Motorcycle Approach Warning (MAW)[20].

C-ITS also has the potential to address conflicts that cannot be detected early due to visual obstructions (e.g., the exemplar cases). The results in Figure 16 indicate that many HO/ODSS, LPV LTAP, and SCP crashes involved a visual obstruction, but there were also other crash configuration groups that did not.

LIMITATIONS

The accuracy of the results are based on a number of assumptions, approximations, and limitations in the data and methods used, many of which are described in [5], [6], [7], [11]. These include the accuracy and representativeness of the MAIDS and MCCS data, as well as the accuracy of the vehicle directional control models used.

SUMMARY/CONCLUSIONS

Pre-crash trajectories have been estimated for 367 crashes involving a light passenger vehicle (LPV) and a motorcycle or moped for the purposes of evaluating the effectiveness and benefits of crash avoidance technologies in avoiding or mitigating these types of crashes. This was accomplished by extending methods and tools to address LPV-PTW crashes. Pre-crash trajectories of 266 cases in the MAIDS database from France, Germany, and Italy and 101 cases in the US MCCS database were reconstructed using a new Motorcycle Automated Accident Reconstruction Tool (M-AART). The resulting pre-crash trajectories of the PTW as viewed from the LPV were broadly distributed in approach angle, with a possible gap from the right rear quadrant (i.e., between the 3 and 6 o'clock directions). The US MCCS data also exhibited a gap between the 10 and 11 o'clock directions. There were relatively few cases where the LPV approached the PTW from the rear (e.g., rear-end).

Further analysis of these estimated pre-crash trajectories indicate that the conflicts begin later, and therefore with smaller TTC values, compared to LPV-LPV crashes that were reconstructed for previous ADAS evaluations. This may be partially due to the smaller length and width of PTWs compared to LPVs, in which LPV-PTW close encounters do not result in a collision, but the same LPV-LPV trajectory would. Therefore LPV-PTW countermeasures may need to address the pre-conflict phase in order to be effective.

It was also observed that 30% of the cases involved a visual obstruction as reported in the crash databases. Many of the cases with a visual obstruction were in the HO/ODSS, LPV LTAP, or SCP crash configuration groups. These cases could potentially be addressed by C-ITS countermeasures such as MAI and MAW.

Only five of the 79 cases in the LPV LTIP, rear end, RTAP/SD, and U-turn crash configuration groups had a coded visual obstruction that contributed to the crash causation. Therefore other factors such as operator distraction and error may be contributing to these types of crashes.

This information can be used to guide further LPV-PTW crash avoidance research, including collecting and analyzing additional on-scene in-depth pre-crash and crash data, field operational experiments, driving simulator experiments, modeling and simulation. The results of this research can potentially help to define requirements for LPV-PTW conflict and crash countermeasures (e.g., BSW, C-ITS) and the development of performance confirmation tests (e.g., New Car Assessment Program (NCAP)). These pre-crash scenarios can also be integrated into the ACAT SIM Crash Sequence Simulation Module in order to estimate the safety benefits and effectiveness of potential countermeasures.

REFERENCES

[1] "Annual Accident Report 2018," European Commission, Directorate General for Transport, June 2018 (https://ec.europa.eu/transport/road_safety/sites/roadsafety/files/pdf/statistics/dacota/asr2018.pdf, accessed 2019-01-18).

[2] "Traffic Safety Facts 2016," DOT HS 812 554, National Highway Traffic Safety Administration, Washington, DC, May 2018 (https://crashstats.nhtsa.dot.gov/Api/Public/ViewPublication/812554, accessed 2018-07-29).

[3] UN ECE, "Consolidated Resolution on the Construction of Vehicles," ECE/TRANS/WP.29/78/Rev.2, United Nations Economic and Social Council, 2011.

[4] Lenkeit, J. F. and Smith, T., "Preliminary Study of the Response of Forward Collision Warning Systems to Motorcycles," Proc. 11th International Motorcycle Conference, Cologne, Germany, October 2016.

[5] Van Auken, R.M., Lenkeit, J., and Smith, T., "Passenger Vehicle-Motorcycle Pre-Crash Trajectory Reconstruction Results based on an Extended Application of the NHTSA-Honda-DRI ACAT Safety Impact Methodology," Paper No. 18-04891, Transportation Research Board Annual Meeting, Washington, DC, January 7-11, 2018.

[6] Van Auken, R.M., Lenkeit, J., and Smith, T., "Passenger Vehicle-Motorcycle Pre-Crash Trajectory Reconstruction and Conflict Analysis Results Based On an Extended Application of the Honda-DRI ACAT Safety Impact Methodology," SAE Technical Paper 2018-01-0510, 2018, doi:10.4271/2018-01-0510.

[7] Van Auken, R.M., Lenkeit, J., and Smith, T., and Kebschull, S, "Passenger Vehicle-Powered Two Wheeler Pre-Crash Trajectory Reconstruction and Conflict Analysis Results for Real-World Crashes in France, Germany, and Italy," Proc. 12th International Motorcycle Conference, Cologne, Germany, October 2018.

[8] MAIDS, "In-Depth Investigations of Accidents Involving Powered Two Wheelers, Final Report 2.0" ACEM, 2009 (http://www.maids-study.eu/pdf/MAIDS2.pdf, accessed 2017-11-13).

[9] Anon., "Motorcycle Crash Causation Study," accomplished by Oklahoma State University, Westat and Dynamic Sciences, Inc. for the FHWA, Turner Fairbank Highway Research Center, McLean, VA, 2016.

[10] OECD, "Motorcycles: Common international methodology for in-depth accident investigations," Organisation for Economic and Community Development, Paris, France, 2008.

[11] Van Auken, R.M., Zellner, J.W., Chiang, D.P., Kelly, J. et al., "Advanced Crash Avoidance Technologies (ACAT) Program – Final Report of the Honda-DRI Team," DOT HS 811 454, National Highway Traffic Safety Administration, Washington, DC, June 2011.

[12] Van Auken, R.M., Lenkeit, J., and Smith, T., "Potential Application of the NHTSA-Honda-DRI ACAT "Safety Impact Methodology" (SIM) to the Evaluation of Automatic Emergency Braking System Effectiveness in Avoiding and Mitigating Collisions with Motorcycles," Paper Number 17-0179, Proc. 25th International Technical Conference on the Enhanced Safety of Vehicles (ESV), Detroit, June 5-8, 2017.

[13] "Fatality Analysis Reporting System (FARS) Analytical User's Manual 1975-2016," DOT HS 812 447, National Highway Traffic Safety Administration, Washington, DC, October 2017.

[14] "Traffic Safety Basic Facts 2018 – Single Vehicle Accidents," European Road Safety Observatory, European Commission, 2018 (https://ec.europa.eu/transport/road_safety/sites/roadsafety/files/pdf/statistics/dacota/bfs2018_single_vehicle_accident.pdf, accessed 2018-06-25).

[15] Neale, V.L. and Dingus, T.A., "Motor Vehicle Warnings," in "Handbook of Warnings," (Mahwah, NY, Lawrence Erlbaum Associates, 2006), 687-700, doi: 10.1177/106480460701500307.

[16] Weir, D.H., Zellner, J.W., and Teper, G.L., "Motorcycle Handling, Volume II: Technical Report," Publication DOT HS 804 191, NHTSA, U.S. Department of Transportation, 1978.

[17] Zellner, J.W. and Weir, D.H., "Moped Directional Dynamics and Handling Qualities," SAE Technical Paper 790260, 1979, https://doi.org/10.4271/790260.

[18] Zellner, J.W., Van Auken, R.M., Silberling, J.Y., Kelly, J., Hagoski, B.K., Sugimoto, Y., and Urai, Y., "Evaluation of a Pre-Production Head-on Crash Avoidance Assist System using an Extended Safety Impact Methodology (SIM)," Paper Number 15-0176, Proc. 24th ESV, Gothenburg, June 2015.

[19] Scanlon, J.M., Sherony, R., Gabler, H.C., "Injury mitigation estimates for an intersection driver assistance system in straight crossing path crashes in the United States," Traffic Injury Prevention, 18:sup1, S9-S17, 2017, DOI: 10.1080/15389588.2017.1300257.

[20] Fischer, H., Kohlinger, O., and Purschwitz, A, "Motorcycles in connected traffic – a contribution to safety", 11th International Motorcycle Conference, Cologne, Germany, October 3, 2016.

CONTACT INFORMATION

R. Michael Van Auken
355 Van Ness Avenue, Suite 200
Torrance, California 90501
United States
RMV@DynRes.com
+1-310-212-5211.

ACKNOWLEDGMENTS

The European Association of Motorcycle Manufacturers (ACEM) provided the MAIDS database. Gratitude is expressed to Antonio Perlot, Veneta Vassileva, and John Paul Peters for their assistance.

Thanks to DRI staff member Paul Satrom for his assistance digitizing the scene diagrams for the M-AART reconstructions.

DEFINITIONS/ABBREVIATIONS

AART	Automated Accident Reconstruction Tool (Honda-DRI ACAT SIM Module 1.3).
ACAT	Advanced Crash Avoidance Technology.
ACEM	European Association of Motorcycle Manufacturers (https://www.acem.eu/).
ADAS	Advanced Driver Assistance Systems.
AEB	Automatic Emergency Braking.
BSW	Blind Spot Warning.
$C(t)$	The estimated state of conflict at time t based on the vehicle positions and velocities at time t. $C(t)$ is true if and only if the vehicles will eventually contact if their velocities remain constant.
CE	Collision Effectiveness – a measure of the ability to avoid a crash.
cg	Center of gravity
C-ITS	Cooperative Intelligent Transportation System.
DRI	Dynamic Research, Inc. (http://www.dynres.com/).
FCW	Forward Collision Warning.
FHWA	US Department of Transportation Federal Highway Administration (https://www.fhwa.dot.gov/).
L1	"A two-wheeled vehicle with an engine cylinder capacity in the case of a thermic engine not exceeding 50 cm^3 and whatever the means of propulsion a maximum design speed not exceeding 50 km/h" as defined in UN/ECE/TRANS/WP.29/78 Rev 2. (i.e., a moped).
L3	"A two-wheeled vehicle with an engine cylinder capacity in the case of a thermic engine exceeding 50 cm^3 or whatever the means of propulsion a maximum design speed exceeding 50 km/h" as defined in UN/ECE/TRANS/WP.29/78 Rev 2. (i.e., a motorcycle).
LPV	Light passenger vehicle, comprising passenger cars, light trucks and vans.
M-AART	A specialized version of the ACAT SIM AART for LPV-PTW crashes.
MAI	Motorcycle Approach Indication, a C-ITS V2V technology.
MAIDS	Motorcycle Accidents In-Depth Study [8] (http://www.maids-study.eu/).
MAW	Motorcycle Approach Warning, a C-ITS V2V technology
MC	Motorcycle (L3 vehicle).
MCCS	Motorcycle Crash Causation Study [9].
NASS	National Automotive Sampling System (https://www.nhtsa.gov/research-data/national-automotive-sampling-system-nass).
NCAP	New Car Assessment Program (e.g., EuroNCAP)
NHTSA	US Department of Transportation National Highway Traffic Safety Administration (https://www.nhtsa.gov/).
OECD	Organisation for Economic Co-operation and Development (https://www.oecd.org/).

POV	Principal other vehicle.
PTW	Powered two wheeler, comprising L1 and L3 vehicles.
SIM	Safety Impact Methodology.
TRCT	Technology Relevant Crash Type.
TTC	Time-to-Collision.
V2V	Vehicle-to-Vehicle [Communications].

APPENDIX A – NASS ACCIDENT TYPES FOR TWO-VEHICLE COLLISIONS

VATYPE and PATYPE Accident Type Codes

Category	Configuration	ACCIDENT TYPES (Includes Intent)		
II. Same Trafficway Same Direction	D. Rear-End	20 → 22, 21, 23 STOPPED 21, 22, 23 ; 24 → 26, 25, 27 SLOWER 25, 26, 27 ; 28 → 30, 29, 31 DECELERATING 29, 30, 31	(EACH - 32) SPECIFICS OTHER	(EACH - 33) SPECIFICS UNKNOWN
	E. Forward Impact	34→35 CONTROL/ TRACTION LOSS ; 36→37 CONTROL/ TRACTION LOSS ; 38→39 AVOID COLLISION WITH VEHICLE ; 40→41 AVOID COLLISION WITH OBJECT	(EACH - 42) SPECIFICS OTHER	(EACH - 43) SPECIFICS UNKNOWN
	F. Sideswipe Angle	44→46 ; 45→45 ; 47	(EACH - 48) SPECIFICS OTHER	(EACH - 49) SPECIFICS UNKNOWN
III. Same Trafficway Opposite Direction	G. Head-On	50→51 LATERAL MOVE	(EACH - 52) SPECIFICS OTHER	(EACH - 53) SPECIFICS UNKNOWN
	H. Forward Impact	54→55 CONTROL/ TRACTION LOSS ; 56→57 CONTROL/ TRACTION LOSS ; 58→59 AVOID COLLISION WITH VEHICLE ; 60→61 AVOID COLLISION WITH OBJECT	(EACH - 62) SPECIFICS OTHER	(EACH - 63) SPECIFICS UNKNOWN
	I. Sideswipe/ Angle	64→65 LATERAL MOVE	(EACH - 66) SPECIFICS OTHER	(EACH - 67) SPECIFICS UNKNOWN
IV. Change Trafficway Vehicle Turning	J. Turn Across Path	68→69 INITIAL OPPOSITE DIRECTIONS ; 70→71, 72→73 INITIAL SAME DIRECTION	(EACH - 74) SPECIFICS OTHER	(EACH - 75) SPECIFICS UNKNOWN
	K. Turn Into Path	77→76, 79→78 TURN INTO SAME DIRECTION ; 80→81, 82→83 TURN INTO OPPOSITE DIRECTIONS	(EACH - 84) SPECIFICS OTHER	(EACH - 85) SPECIFICS UNKNOWN
V. Intersecting Paths (Vehicle Damage)	L. Straight Paths	87→86 ; 88→89	(EACH - 90) SPECIFICS OTHER	(EACH - 91) SPECIFICS UNKNOWN
VI. Miscellaneous	M. Backing Etc.	92→93 OTHER VEHICLE OR OBJECT BACKING VEHICLE	98 OTHER ACCIDENT TYPE 99 UNKNOWN ACCIDENT TYPE 00 NO IMPACT	

Source: NASS GES Analytical User's Manual, 1998-2000.

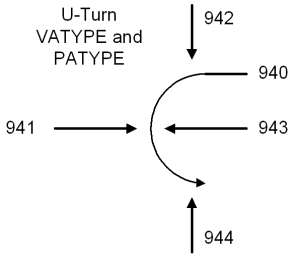

APPENDIX B – PRECRASH TRAJECTORIES AND CONFLICTS BY CRASH CONFIGURATION GROUP

The estimated pre-crash trajectories and conflicts for the 3 sec prior to impact are illustrated in Figures A1 through A24 for the 24 crash configuration groups defined in Table 2. The graph on the left side of each figure depicts the position of the PTW relative the LPV in the LPV frame, and is a subset of the cases depicted in Figure 7. The graph on the right side of each figure depicts the position of the LPV relative to the PTW in the PTW frame, and is a subset of the cases depicted in Figure 8. The yellow highlighting indicates the positions that are in a state of conflict defined herein as $C(t) = \text{true}$.

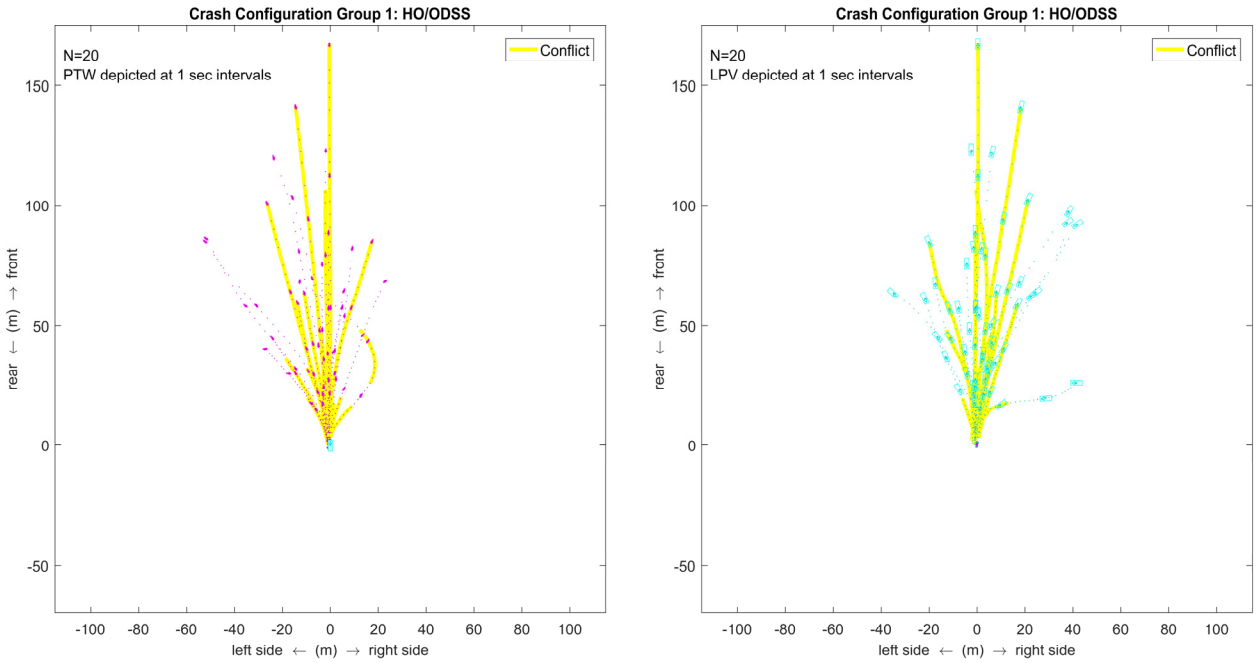

Figure B1. Head-on or opposite direction side swipe

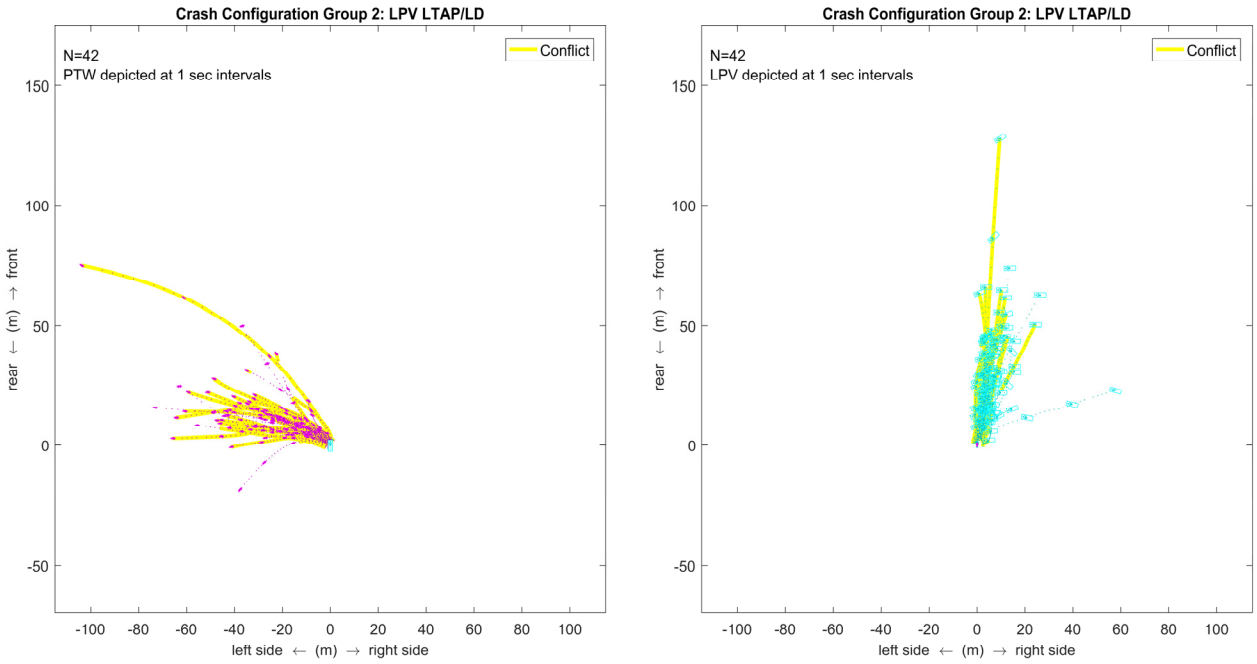

Figure B2. LPV left turn across PTW path/lateral direction

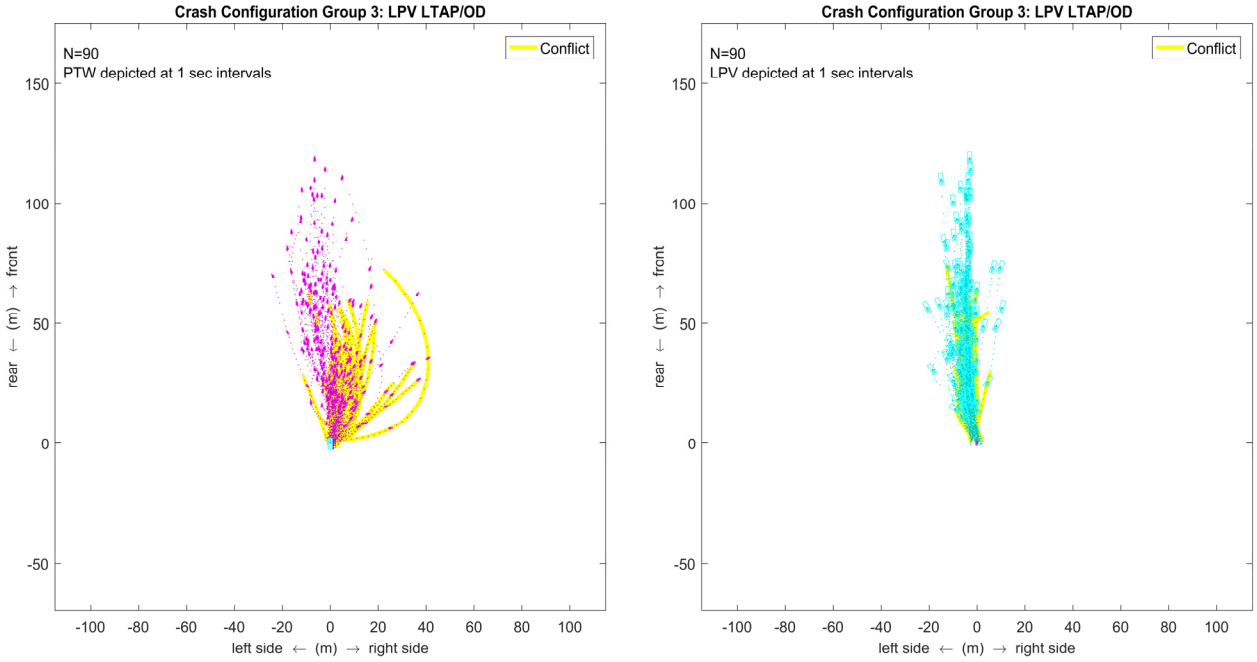

Figure B3. LPV left turn across PTW path/opposite direction

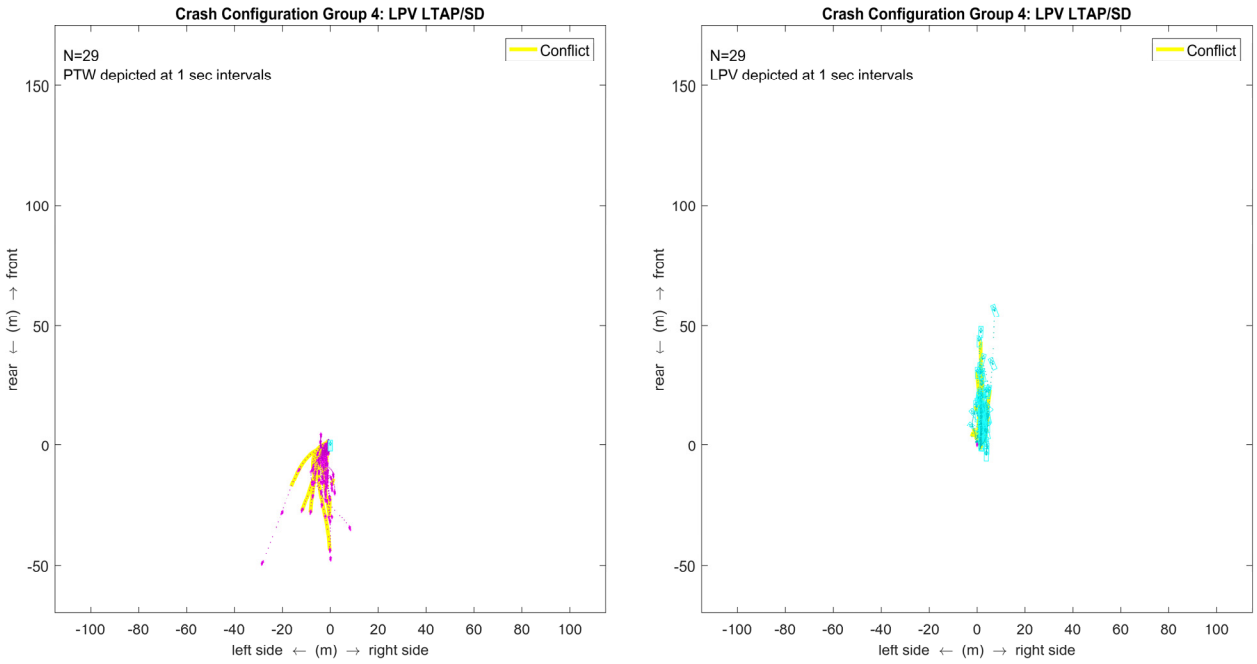

Figure B4. LPV left turn across PTW path/same direction

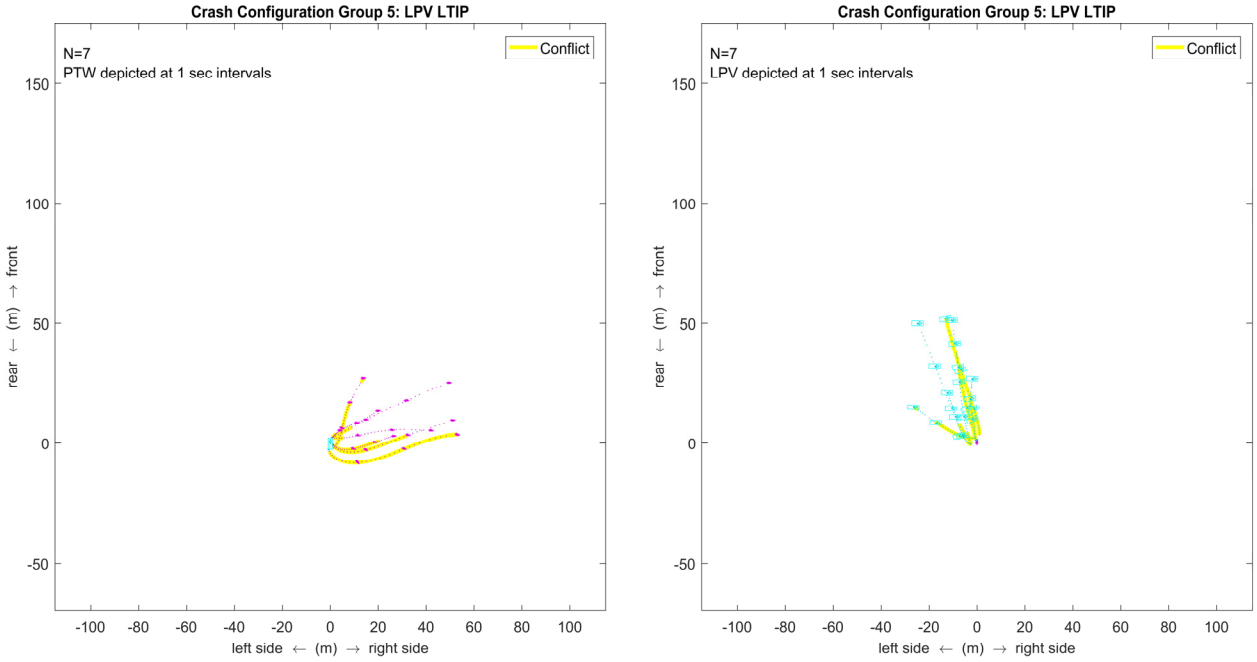

Figure B5. LPV left turn into PTW path

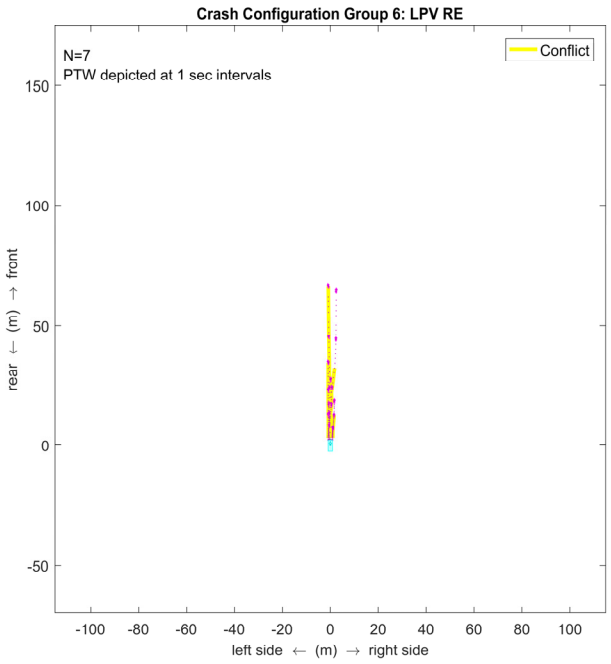

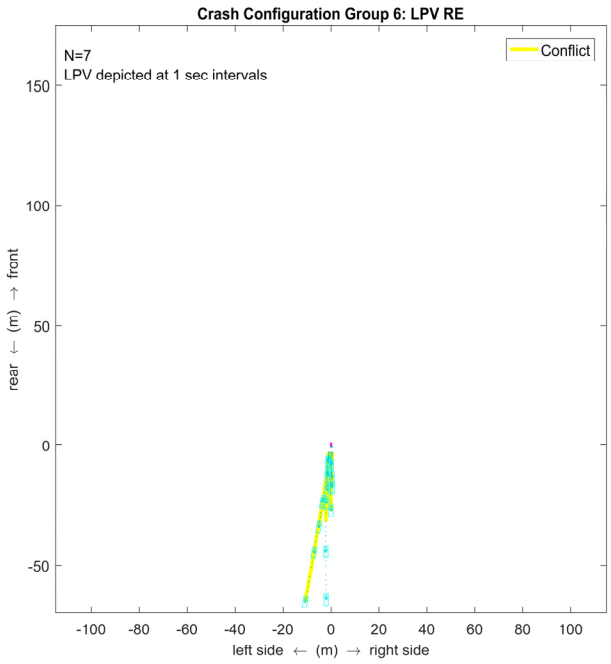

Figure B6. LPV rear-end PTW

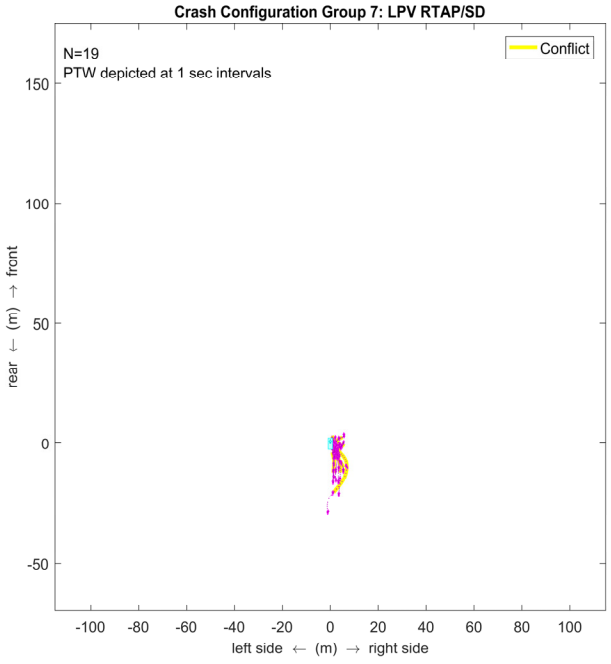

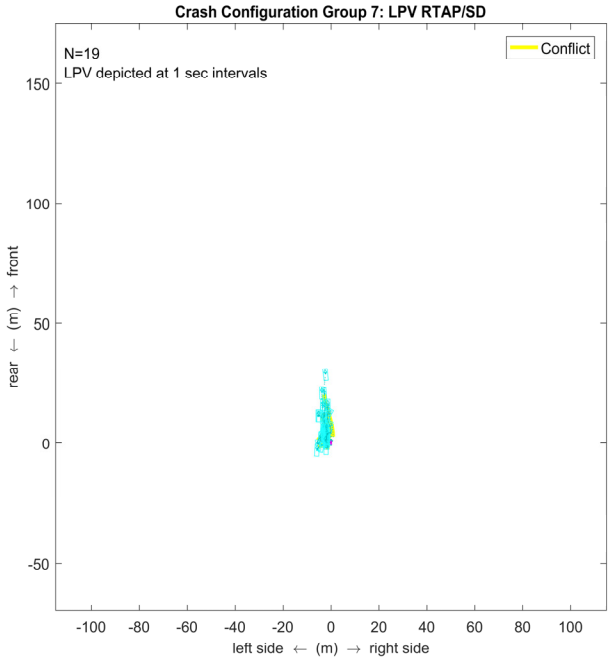

Figure B7. LPV right turn across path/same direction

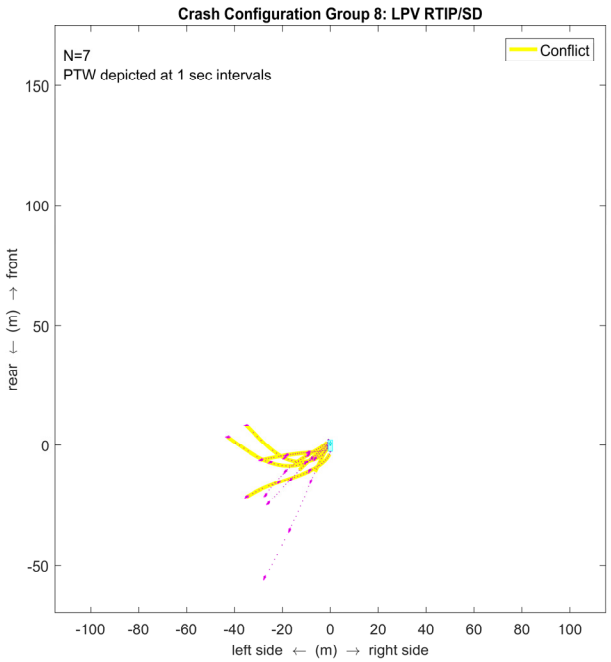

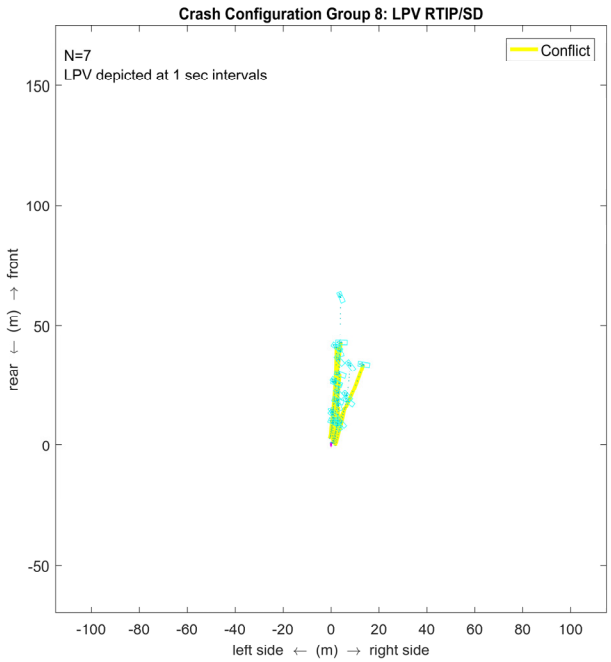

Figure B8. LPV right turn into path/same direction

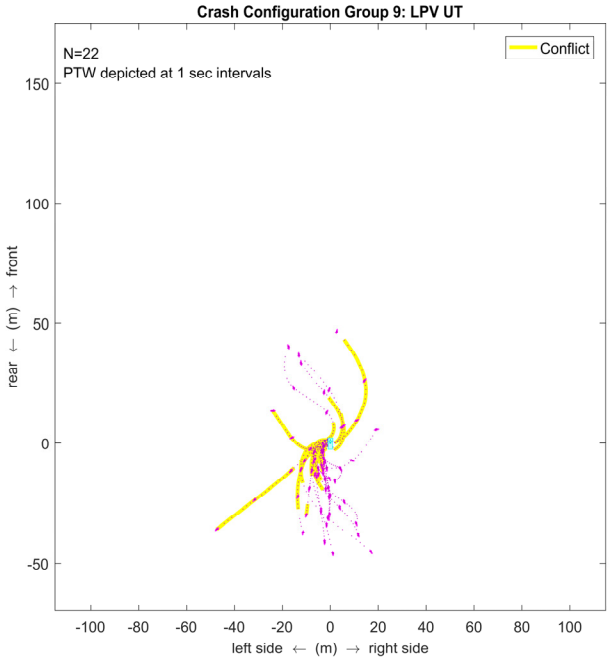

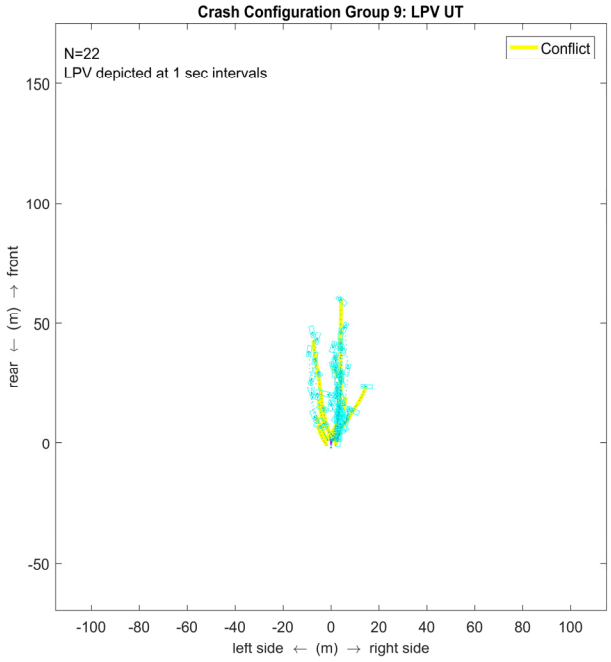

Figure B9. LPV U-turn across PTW path

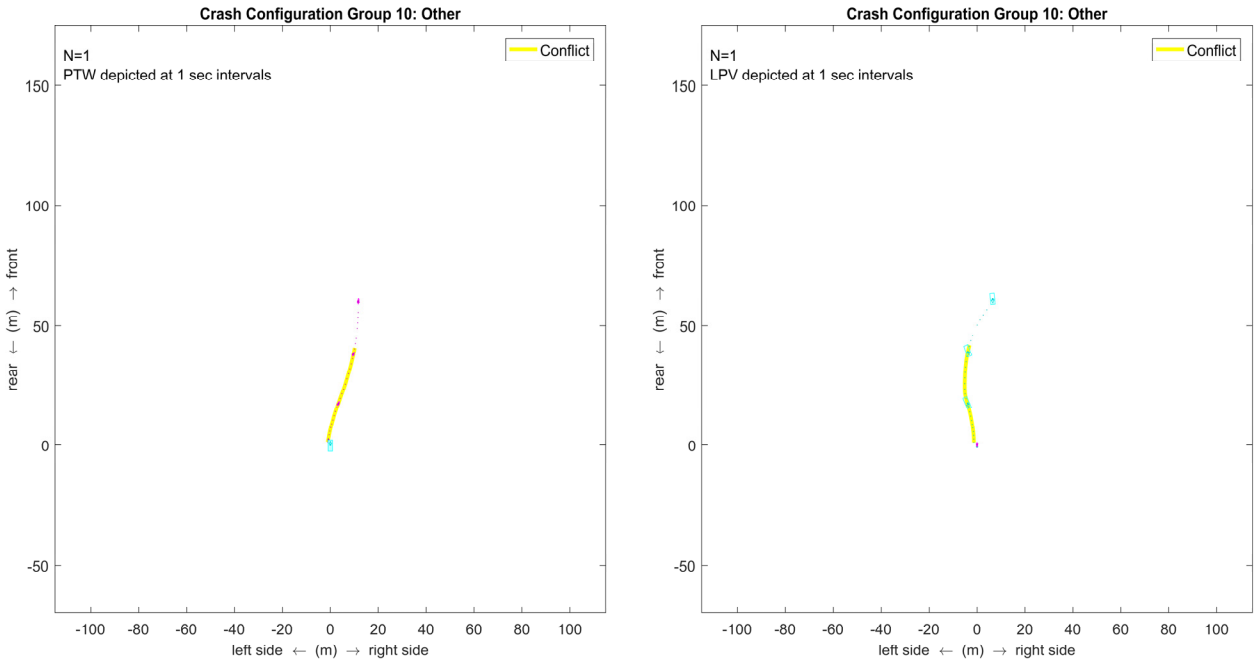

Figure B10. Other crash type

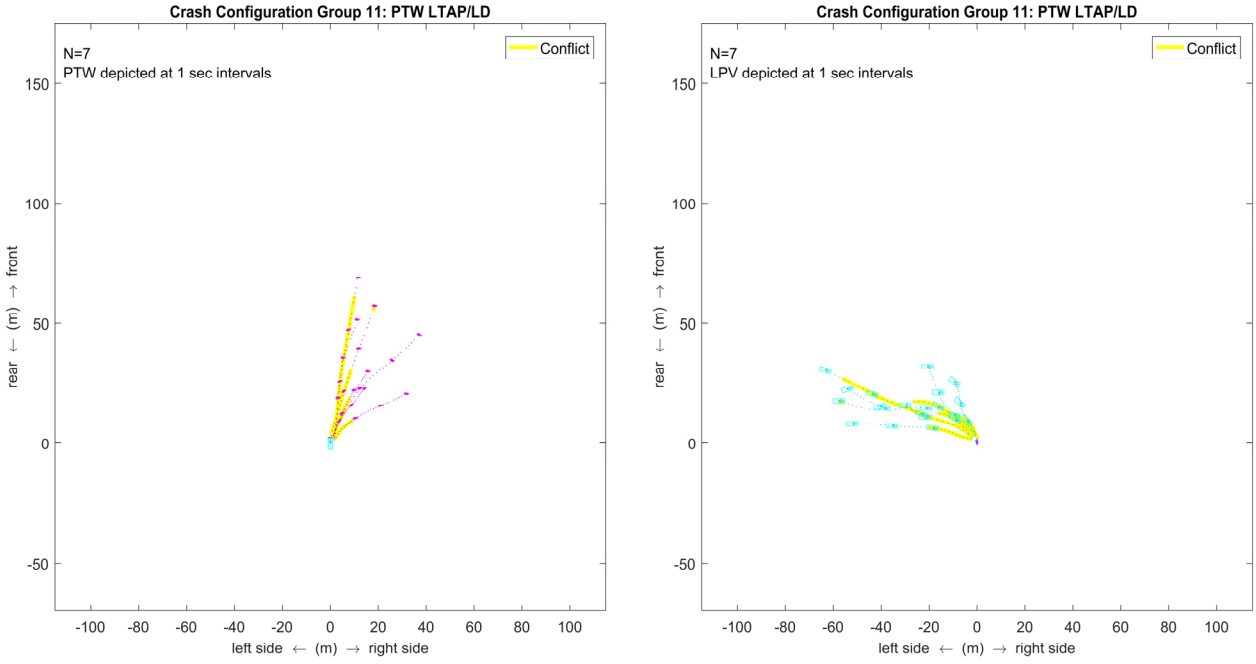

Figure B11. PTW left turn across LPV path/lateral direction

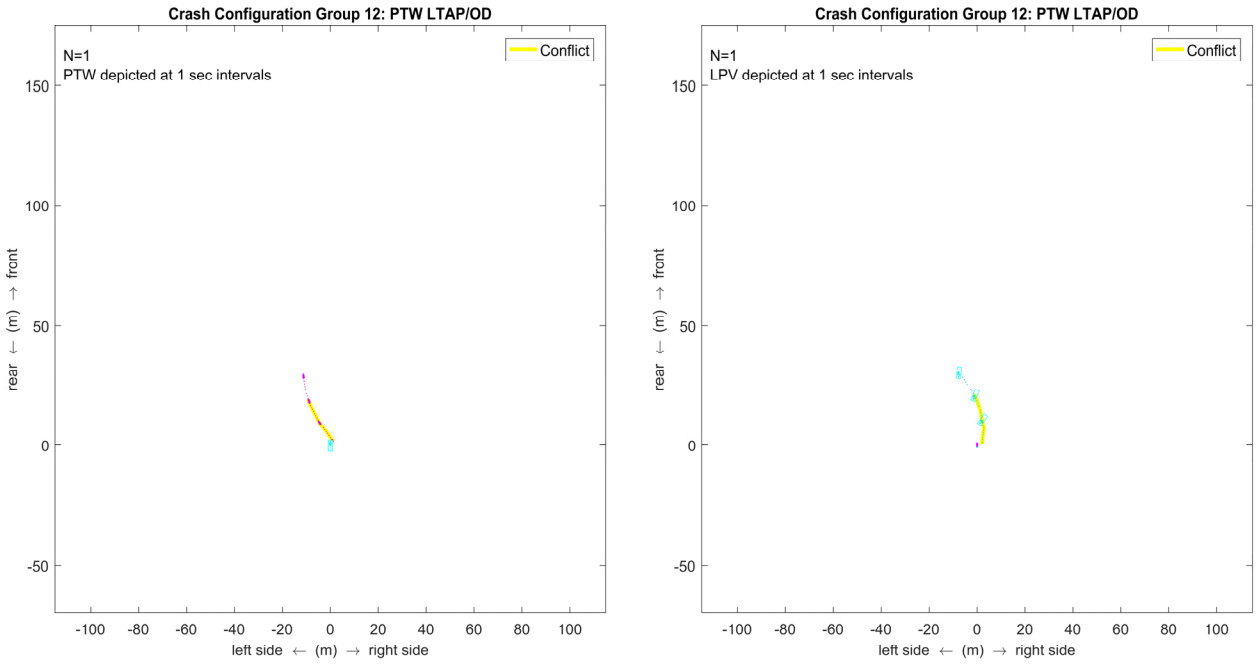

Figure B12. PTW left turn across LPV path/opposite direction

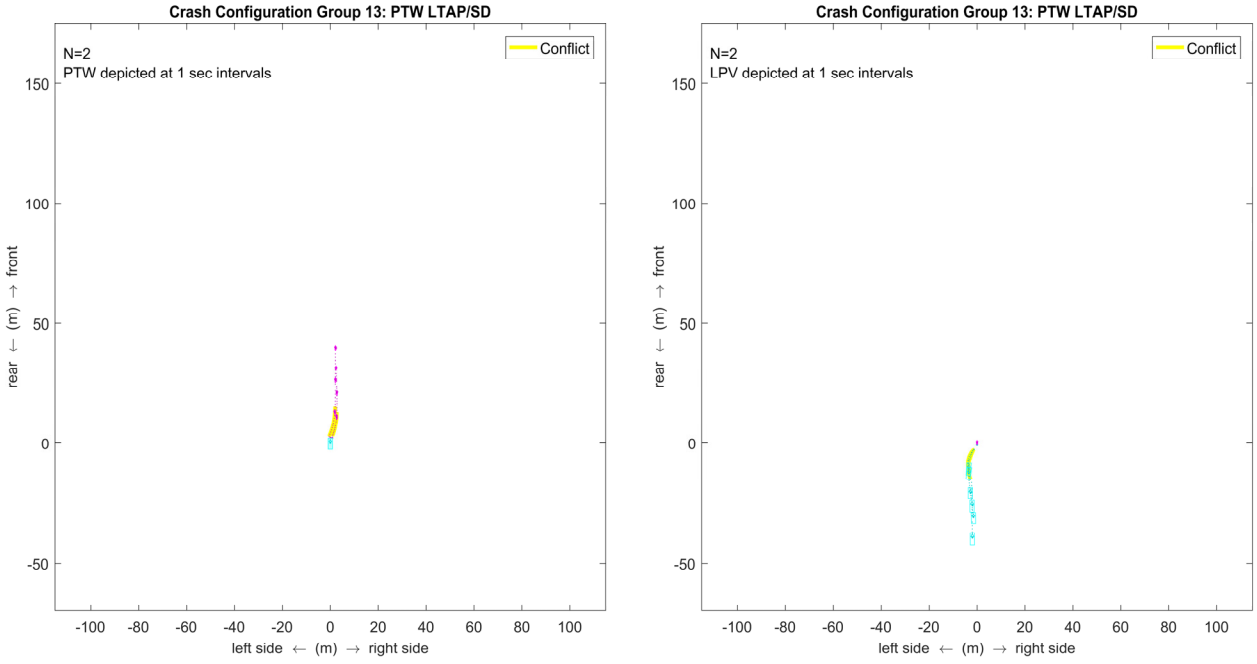

Figure B13. PTW left turn across LPV path/same direction

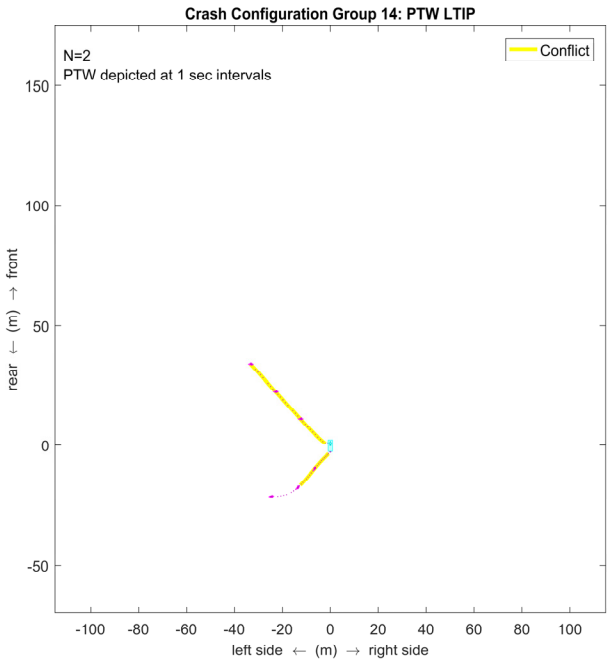

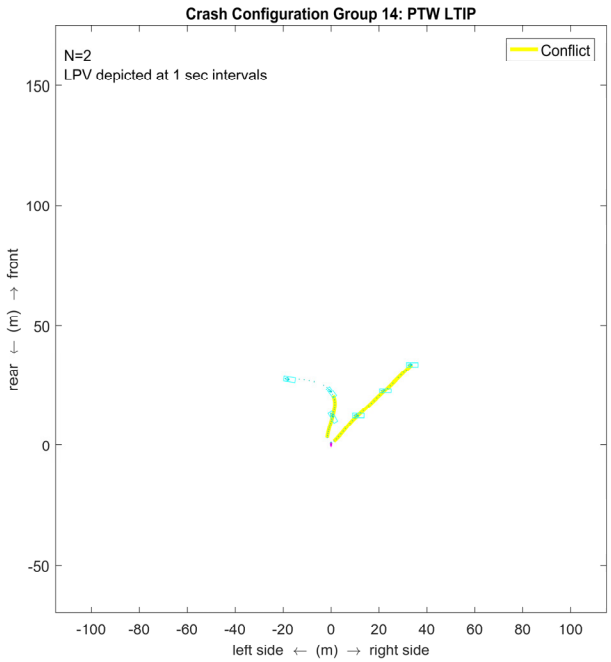

Figure B14. PTW left turn into LPV path

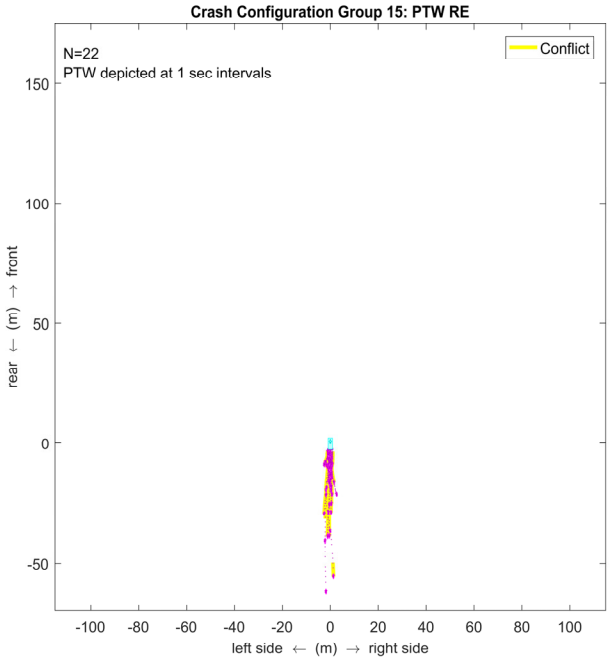

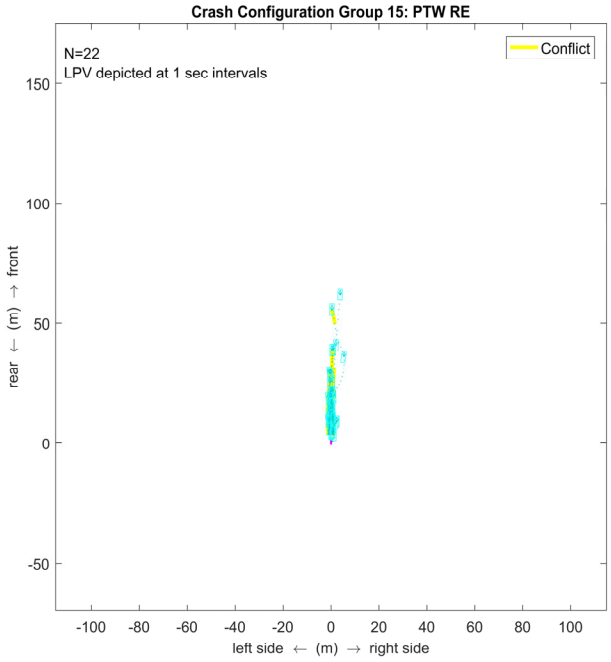

Figure B15. PTW rear-end LPV

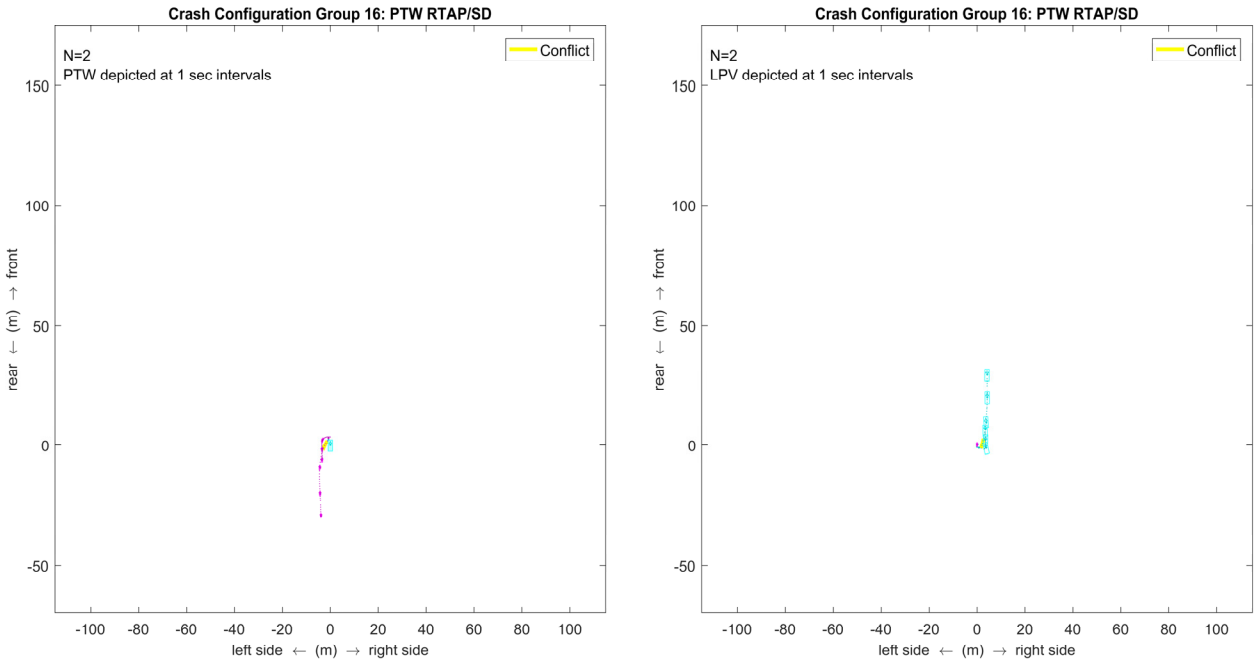

Figure B16. PTW right turn across LPV path/same direction

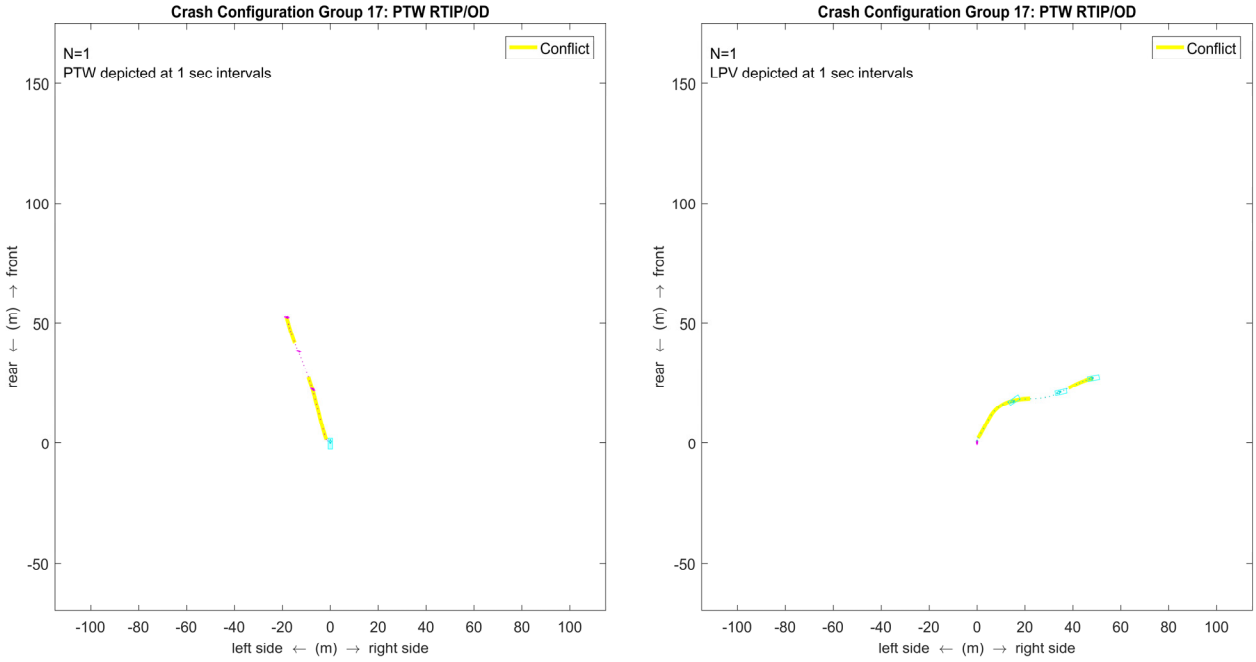

Figure B17. PTW right turn into LPV path/opposite direction

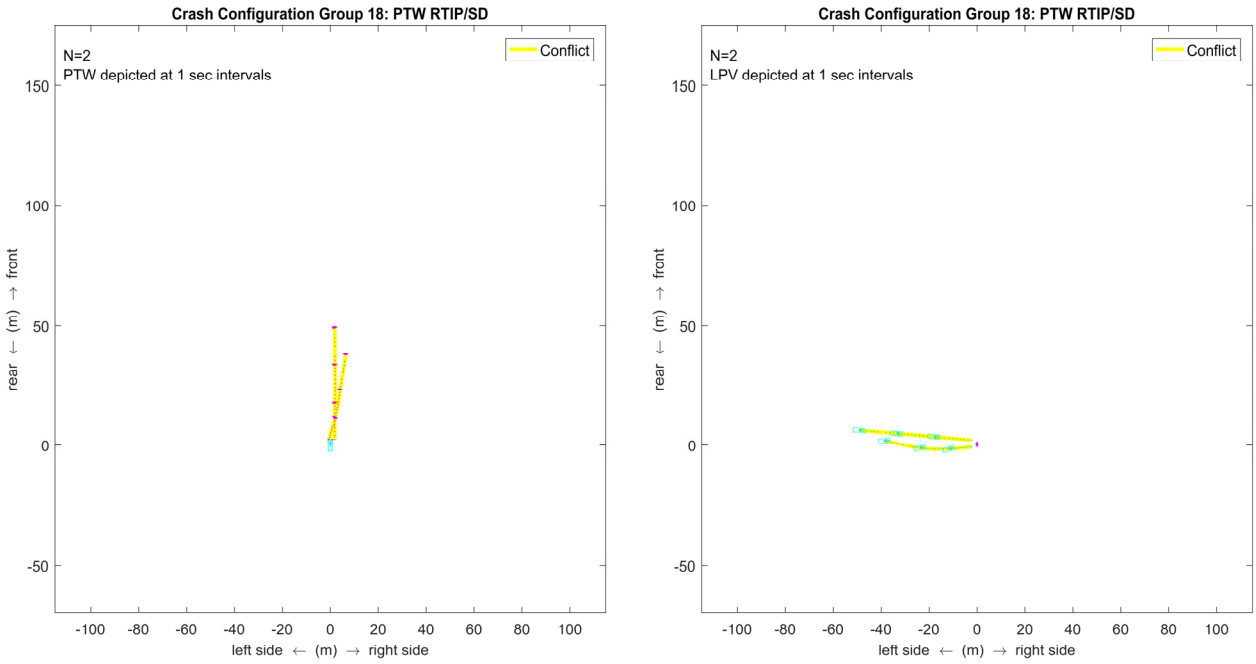

Figure B18. PTW right turn into LPV path/same direction

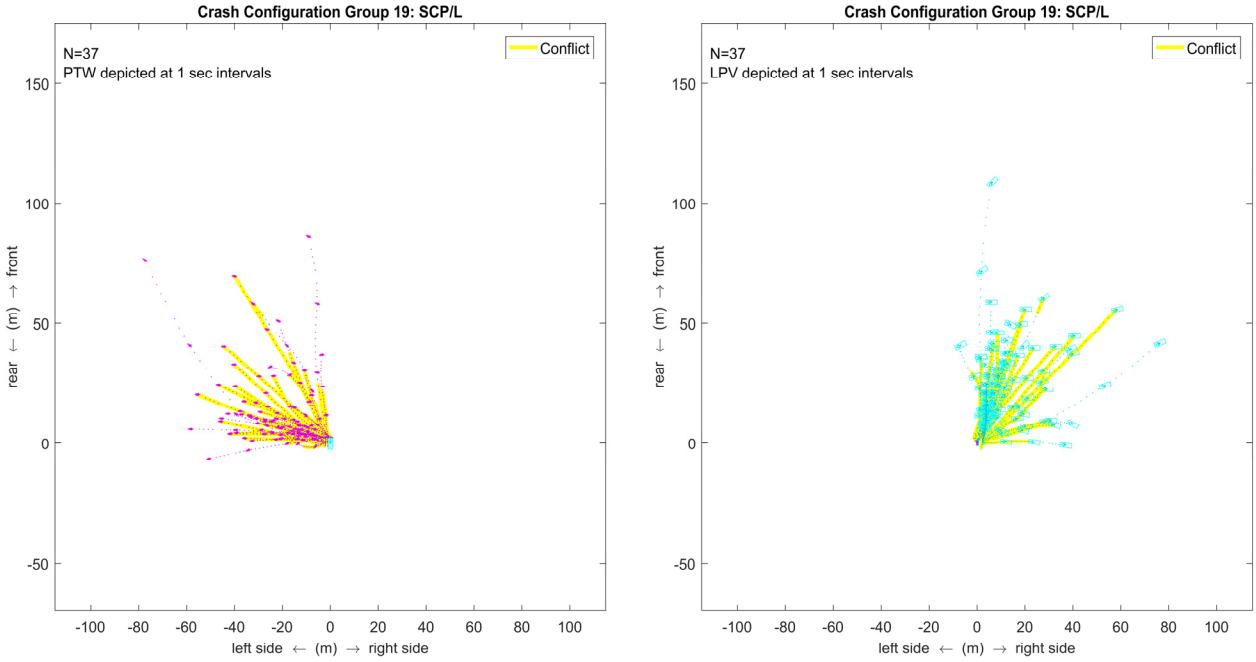

Figure B19. Straight crossing path/PTW on left side of LPV

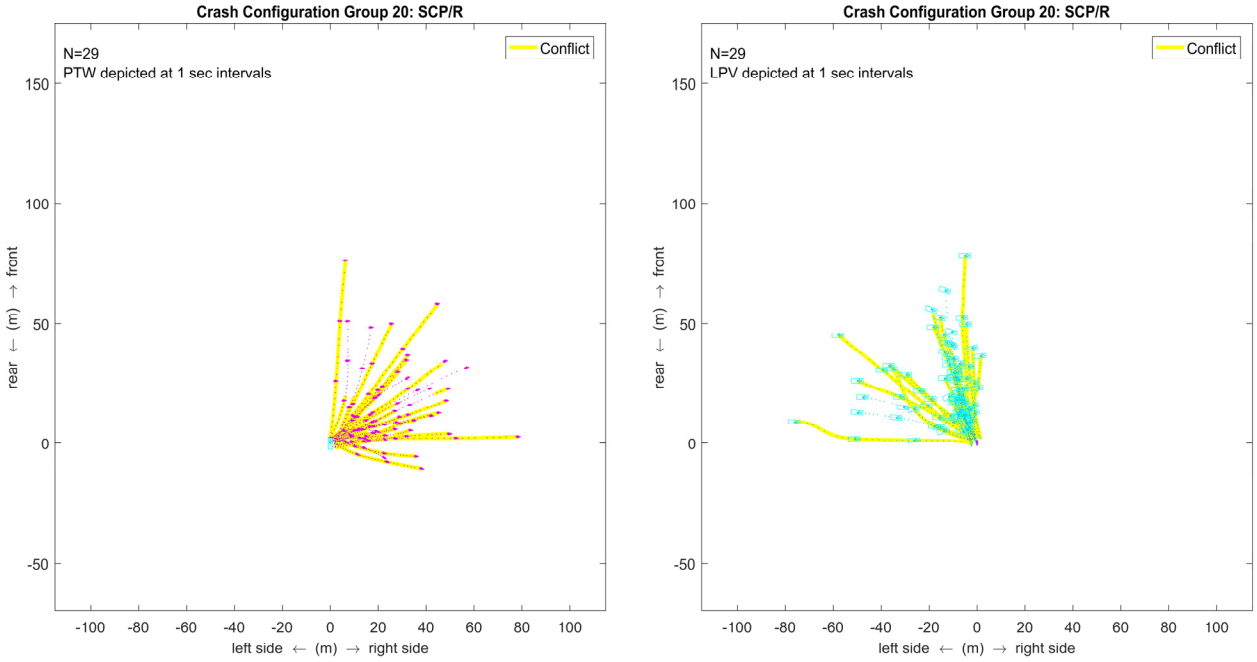

Figure B20. Straight crossing path/PTW on right side of LPV

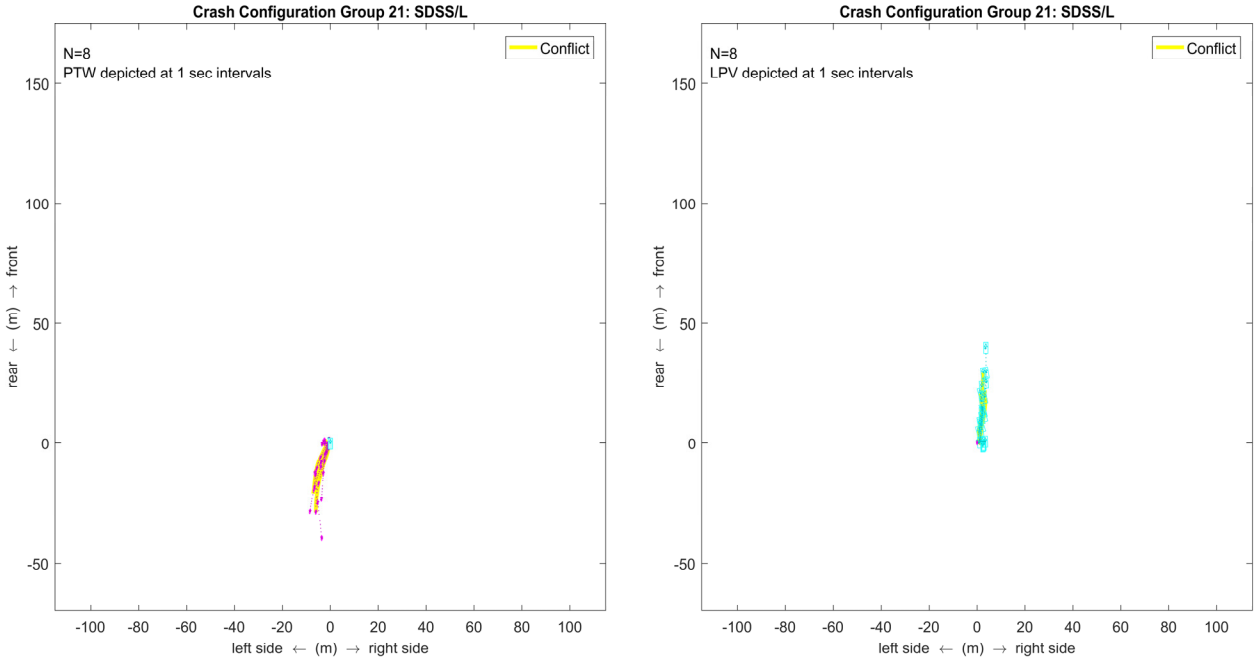

Figure B21. Same direction side swipe/PTW on the left side of LPV

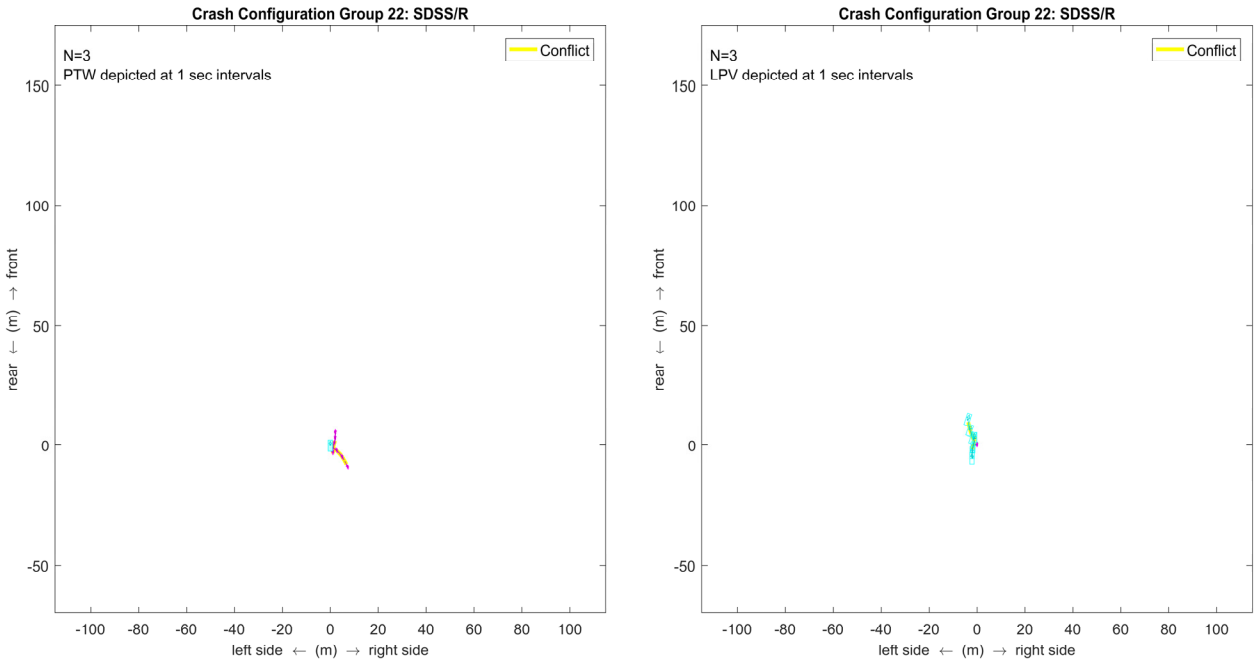

Figure B22. Same direction side swipe/PTW on the right side of LPV

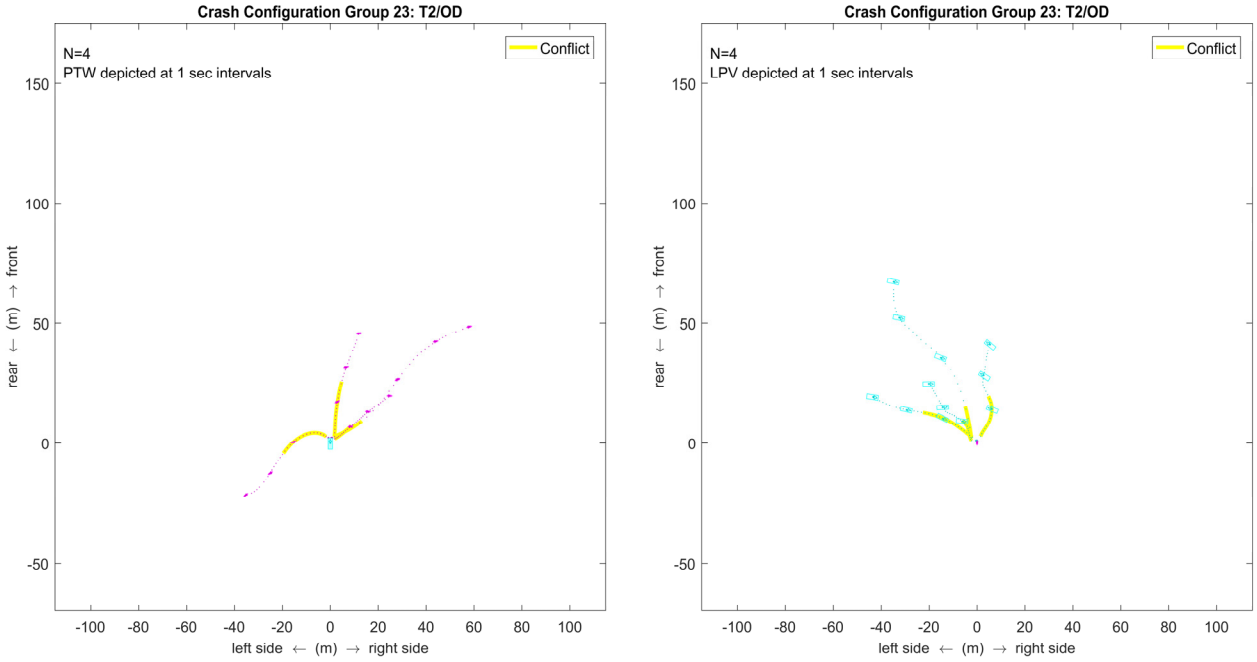

Figure B23. Both vehicles turning/opposite direction

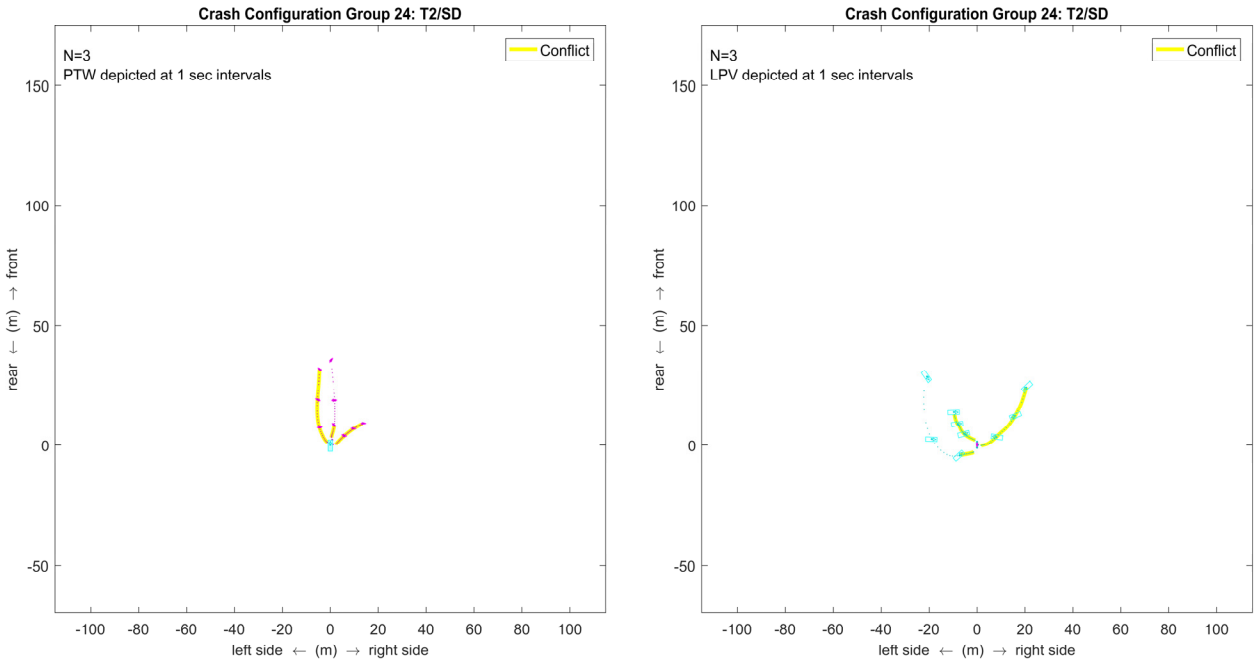

Figure B24. Both vehicles turning/same direction